Cell

A Calmodulin-Dependent Translocation Pathway for Small Secretory Proteins

Sichen Shao[1,2,3] and Ramanujan S. Hegde[1,3,*]
[1]Cell Biology and Metabolism Program, National Institute of Child Health and Human Development, 18 Library Drive, Building 18, Room 101, National Institutes of Health, Bethesda, MD 20892, USA
[2]Department of Biology, Johns Hopkins University, 3400 North Charles Street, Baltimore, MD 21218, USA
[3]Present address: MRC Laboratory of Molecular Biology, Hills Road, Cambridge, CB2 0QH, UK
*Correspondence: rhegde@mrc-lmb.cam.ac.uk
DOI 10.1016/j.cell.2011.11.048

SUMMARY

Metazoans secrete an extensive array of small proteins essential for intercellular communication, defense, and physiologic regulation. Their synthesis takes mere seconds, leaving minimal time for recognition by the machinery for cotranslational protein translocation into the ER. The pathway taken by these substrates to enter the ER is not known. Here, we show that both in vivo and in vitro, small secretory proteins can enter the ER posttranslationally via a transient cytosolic intermediate. This intermediate contained calmodulin selectively bound to the signal peptides of small secretory proteins. Calmodulin maintained the translocation competence of small-protein precursors, precluded their aggregation and degradation, and minimized their inappropriate interactions with other cytosolic polypeptide-binding proteins. Acute inhibition of calmodulin specifically impaired small-protein translocation in vitro and in cells. These findings establish a mammalian posttranslational pathway for small-protein secretion and identify an unexpected role for calmodulin in chaperoning these precursors safely through the cytosol.

INTRODUCTION

The first step in eukaryotic protein secretion is translocation into the endoplasmic reticulum (ER). In metazoans, this process usually begins when the signal recognition particle (SRP) recognizes the hydrophobic N-terminal signal sequence of a secretory protein as it emerges from the ribosome (Shan and Walter, 2005). An interaction between SRP and the SRP receptor facilitates targeting of the ribosome-nascent chain complex to the ER, where the ribosome docks onto the Sec61 protein-conducting channel (Osborne et al., 2005). Subsequent translocation is coupled to translation, with the polypeptide passing through the Sec61 channel as it emerges from the ribosomal exit tunnel. The signal sequence is removed during translocation and the translocated mature domain then traffics through the secretory pathway for extracellular secretion. This cotranslational translocation pathway is conserved from bacteria to mammals and is used by most secretory and membrane proteins (Rapoport, 2007).

However, secretory proteins smaller than ~100 residues (Table S1 available online) might complete translation before efficient cotranslational targeting (Goder et al., 2000; Zimmermann and Mollay, 1986; Zimmermann et al., 1990). This is due to a limited amount of time between when the signal sequence is available for SRP recognition and when the termination codon is reached. Whether such short proteins can access the cotranslational pathway therefore depends on whether this time window is sufficient for SRP recognition, targeting to its receptor, transfer to the Sec61 translocon, and insertion into the channel. If this window is too short, then small proteins would be released into the cytosol and need to enter the ER posttranslationally, a process that is poorly understood in metazoans.

Thus, a decisive question in understanding short protein biosynthesis is whether targeting can reasonably occur during its synthesis. Direct estimates of targeting kinetics in vivo suggest that an average of ten seconds is needed to target even a highly robust SRP-dependent signal (Goder et al., 2000). This means that after a signal sequence first emerges from the ribosome at ~60 residues of synthesis (Figure S1A), targeting may not occur for another ~60 residues (assuming translation at 6 residues/sec). A significant proportion of proteins shorter than ~120 residues would therefore terminate translation before they are targeted. While selective mRNA localization or exceptionally strong translational arrest could conceivably overcome these temporal constraints (Figure S1B), these potential mechanisms are poorly characterized. Thus, short precursors may well need to use posttranslational translocation to enter the ER efficiently.

Posttranslational ER translocation has been most extensively studied in yeast (Panzner et al., 1995b), where the pathway is utilized by secretory proteins containing modestly hydrophobic signal sequences that cannot engage SRP effectively (Ng et al., 1996). In this pathway, it is thought that general cytosolic chaperones, most notably of the Hsp70 family, interact with and maintain translocation competence of fully-synthesized substrates in the cytosol (Chirico et al., 1988; Deshaies et al., 1988). Upon release from the chaperones, substrates engage the heptameric Sec complex at the ER. This translocon is

composed of the Sec61 complex associated with the Sec62/63/71/72 complex (Deshaies et al., 1991; Panzner et al., 1995a). Substrates that enter the Sec translocon are made accessible to lumenal Kar2 (an Hsp70 family member), which, via cycles of ATPase-driven binding and release, "ratchets" the polypeptide across the membrane (Brodsky and Schekman, 1993; Matlack et al., 1999; Panzner et al., 1995a). Thus, the general paradigm is one of substrate chaperoning in the cytosol, engagement of a membrane-bound channel, and biased translocation via a lumenal polypeptide-binding protein.

Although all of the components in this pathway are conserved in mammals, such posttranslational translocation has not been studied extensively. Notably, classical yeast posttranslational substrates, such as prepro-α-factor, can only translocate cotranslationally across mammalian ER membranes (Garcia and Walter, 1988). It was therefore surmised that in higher eukaryotes, the SRP-dependent cotranslational pathway predominantes and has evolved to accommodate a wider range of substrates than in yeast. The main posttranslational models analyzed thus far in mammalian systems have been short secreted proteins (Schlenstedt and Zimmermann, 1987; Schlenstedt et al., 1992; Zimmermann and Mollay, 1986). While they were observed to translocate posttranslationally in vitro, the cellular machinery and mechanisms involved have been unclear. Here, we demonstrate that both in vivo and in vitro, a substantial proportion of short secretory proteins normally utilize posttranslational translocation to enter the ER. Mechanistic analysis of this pathway in vitro revealed a conceptually similar logic to the yeast posttranslational system. However, we discovered an unexpected function for calmodulin in recognizing short protein precursors and chaperoning them through the cytosol. Remarkably, calmodulin's role in protecting short proteins from irreversible off-pathway fates such as ubiquitination and aggregation could not be fully compensated by other cytosolic chaperones.

RESULTS AND DISCUSSION

Development of an Assay to Detect Posttranslational Translocation

To determine whether posttranslational translocation occurs in mammalian cells under physiologically normal conditions, we developed an assay to detect a putative cytosolic translocation intermediate with high specificity and sensitivity. To do this, we determined whether a 15-residue biotin acceptor epitope (BioTag) near the C terminus of a short protein was accessible to cytosolic biotin ligase (BirA) before its translocation into the ER (Figure 1A). Because the BioTag epitope would be deep inside the ribosome when the termination codon is reached, cotranslational (i.e., ribosome-coupled) translocation would preclude its access to BirA. By contrast, a biotinylated signal-cleaved product would be a signature of posttranslational translocation that necessarily involved a BirA-accessible cytosolic intermediate.

Our model short protein was Cecropin A (CecA), a secreted antimicrobial peptide derived from a 64-residue precursor. Prolactin (Prl) served as a well-established cotranslationally translocated model. Each protein was modified to contain a BioTag-HA epitope (Figure 1B) and the experimental strategy was characterized in vitro. When synthesized in rabbit reticulocyte lysate (RRL), the BioTagged version of CecA could be site-specifically biotinylated by BirA as evidenced by its pull-down with immobilized avidin (Figure 1C, downward arrowhead). Biotinylation was dependent on both the BioTag and BirA.

When CecA translation reactions were incubated with ER-derived rough microsomes (RMs), CecA was translocated into the lumen as judged by both signal sequence cleavage and protease protection (Figure 1D). Biotinylated CecA was translocated comparably to nonbiotinylated CecA (Figure 1E, upward arrowhead), illustrating that the small biotin moiety does not preclude translocation. Cytosolic BirA could not access the substrate after translocation into the ER (Emerman et al., 2010; data not shown), confirming that biotinylation is cytosol-specific.

A similar analysis of BioTagged Prl showed that in the cytosol, it was biotinylated in a BirA-dependent manner (Figure 1F, downward arrowhead). Inclusion of RMs during Prl translation resulted in its cotranslational translocation into the lumen, as evidence by its signal cleavage. However, inclusion of BirA during Prl translocation resulted in biotinylation of only the non-translocated population (Figure 1F). Thus, when the ribosome is coupled to the translocon during translocation, the nascent chain is not accessible to BirA in the cytosol. Collectively, these results establish a minimally perturbing, orthogonal, and site-specific modification that can be used to 'mark' a putative cytosolic intermediate without precluding its subsequent translocation.

Posttranslational Translocation in Mammalian Cells

The biotinylation assay was imported into mammalian cells and the behavior of CecA was analyzed. In pulse-labeled HeLa cells, a signal-cleaved and biotinylated form of BioTagged CecA was observed (Figure 1G; upward arrowhead). This product was not released by selective plasma membrane permeabilization with digitonin (Figure S1C), confirming its noncytosolic location. CecA had therefore entered the ER (i.e., was signal cleaved), after having been exposed to the cytosol (i.e., was biotinylated). Biotinylation required BirA and was observed in other cell types (Figure S1D). In contrast, BioTagged Prl was efficiently translocated, but not biotinylated (Figure 1H), as expected for a cotranslationally translocated protein. Thus, CecA can enter the mammalian secretory pathway posttranslationally via a cytosolic intermediate.

Signal sequence swapping experiments showed that both length and signal sequence features influence access to post-translational translocation. The Prl signal sequence fused to the CecA mature domain (Prl-CecA) supported translocation (as judged by signal cleavage), but little if any of the translocated product was biotinylated (Figure 1G and Figures S1D and S1E). When the proteasome was inhibited, biotinylated Prl-CecA precursor was detected (Figure 1G and Figure S1E). Thus, the highly efficient cotranslational signal sequence from Prl cannot fully overcome the short kinetic window for SRP-mediated targeting of a small protein. However, even when Prl-CecA precursor was prevented from degradation, biotinylated signal-cleaved protein was not observed, suggesting that Prl-CecA is not an efficient posttranslational translocation substrate.

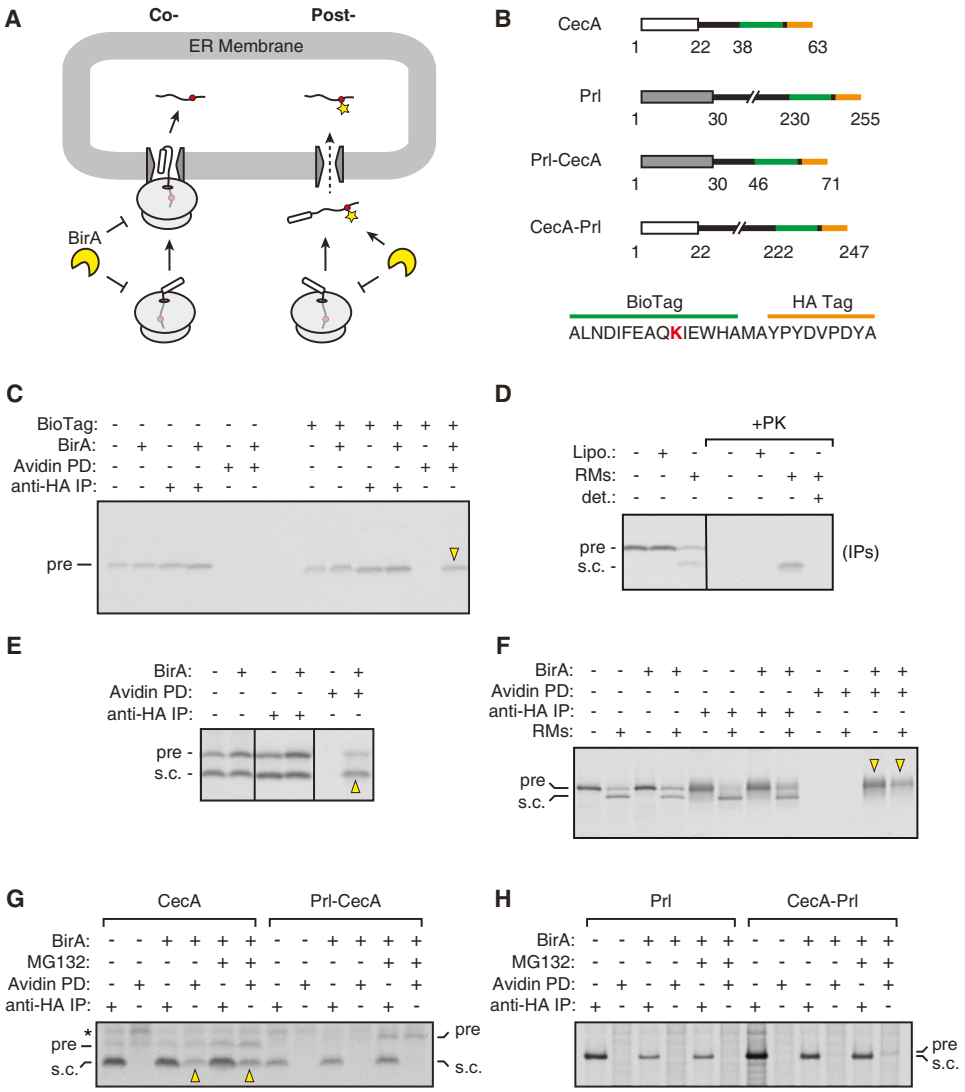

Figure 1. Small Proteins Enter the Mammalian ER Posttranslationally

(A) Experimental strategy to discriminate ribosome-coupled cotranslational translocation (left) from posttranslational translocation (right). A biotin ligase (BirA) can add biotin (star) to an acceptor sequence (red) only if it is exposed to the cytosol.

(B) Diagram of constructs used for translocation assays. The C-terminal tag replaces a segment of the substrate, rather than adding to the end.

(C) CecA without or with the BioTag sequence was translated in vitro in the absence or presence of recombinant BirA. The samples were either analyzed directly, or after anti-HA immunoprecipitation (IP) or avidin pulldown (PD). Arrowhead is biotinylated product.

(D) CecA was synthesized in native rabbit reticulocyte lysate (N-RRL) and posttranslationally incubated with either buffer, liposomes (Lipo.), or ER-derived rough microsomes (RMs). The samples were then analyzed directly or digested with proteinase K (PK) in the absence or presence of detergent (det.). The PK-digested samples were immunoprecipitated to recover the CecA prior to analysis. Precursor (pre) and signal-cleaved (s.c.) products are indicated.

(E) CecA was synthesized in N-RRL in the absence or presence of BirA and posttranslationally incubated with RMs. The samples were either analyzed directly, or after anti-HA IP or avidin PD. Arrowhead indicates biotinylated translocated product.

(F) BioTagged Prl was translated in the absence or presence of recombinant BirA and/or RMs and analyzed directly or subjected to anti-HA IP or avidin PD.

(G and H) BioTagged constructs were coexpressed without or with BirA in HeLa cells, pulse labeled for 1 hr, and subjected to anti-HA IP or avidin PD. Proteasome inhibitor (MG132) was included during the labeling where indicated. Yellow arrowheads show biotinylated translocated product. Asterisk indicates a nonspecific product.

See also Figure S1.

The CecA signal sequence fused to the Prl mature domain (CecA-Prl) was also translocated, but none of the signal-cleaved product was observed to be biotinylated (Figure 1H). Biotinylated CecA-Prl precursor was detected with proteasome inhibition, indicating that it is capable of being biotinylated in the cytosol. Thus, both Prl-CecA and CecA-Prl primarily enter the ER cotranslationally, with cytosolically released precursor being degraded by the proteasome instead of being

translocated posttranslationally. Posttranslational translocation is therefore neither solely encoded in the signal sequence, nor simply a consequence of short precursors. Instead, CecA has evolved a signal sequence that, while sub-optimal for the cotranslational pathway, allows its short passenger to avoid cytosolic quality control (Figure S1E) and engage a yet uncharacterized but specific posttranslational translocation pathway. Comparing the relative amounts of biotinylated precursor and translocated product (Figure 1G and Figure S1E), we estimate that at least ~35% of CecA translocates posttranslationally in mammalian cells. This is probably an underestimate, since biotinylation is not likely to be 100% efficient given the transient nature of the cytosolically accessible intermediate. Thus, in vivo under normal physiological conditions, posttranslational translocation is a substantial mechanism for small-protein entry into the ER.

Reconstitution of Posttranslational Translocation In Vitro

To mechanistically dissect this posttranslational translocation pathway, we studied the process in a reconstituted mammalian in vitro system. Epitope-tagged CecA precursor was synthesized in RRL, further translation was prevented by either removing ribosomes or adding RNase, and the reaction was posttranslationally incubated with RMs. Translocation was assayed by signal sequence cleavage and protease protection assays, while protein interactions were detected by sucrose gradient size fractionation and chemical crosslinking (Figure 2A). In our initial studies, posttranslational translocation was inefficient (~10%–30% at best; data not shown), similar to previous findings (Schlenstedt et al., 1990, 1992). Size fractionation and crosslinking studies of the translation products showed that the substrate engaged many different cytosolic complexes of heterogeneous size, only a subset of which were even modestly translocation-competent (Figure 2B). Because low-level translocation precluded any substantive mechanistic dissection, we first optimized the system to improve homogeneity of functional CecA complexes and maximize its translocation.

Among the conditions tested, a nonnucleased "native" RRL (N-RRL) translation system proved superior. CecA precursor synthesized in N-RRL was substantially more homogeneous on sucrose gradients (Figure 2C), with nearly all of the CecA migrating in a few fractions near the top (<60 kD) region of the gradient (Figure 2D). Crosslinking analysis also showed much more homogeneity, revealing a single ~20 kD interaction partner (Figure 2C). Importantly, testing of these CecA-containing fractions for translocation revealed markedly improved efficiency of ~60%. Two other short secretory proteins also showed comparably homogenous migration in the same part of the sucrose gradient, and these fractions were active in posttranslational translocation (Figure S2).

With this improved system, we used the BirA-BioTag assay system to determine if the posttranslational pathway is used under conditions where the cotranslational pathway is available. CecA translated in N-RRL supplemented with RMs and BirA was observed to be efficiently translocated (Figure 2E). Avidin pulldowns revealed that the translocated population was biotinylated, indicating that the BioTag was accessible to cytosolic BirA before translocation. Because the BioTag is near the C terminus of CecA, we can further conclude that CecA must have terminated translation and emerged from the ribosome before its translocation. Consistent with this conclusion, inactivation of the cotranslational pathway by mild trypsin digestion of RMs had no effect on CecA translocation (data not shown). Additional experiments testing Prl-CecA and CecA-Prl in N-RRL confirmed that posttranslational translocation is both length and signal sequence dependent (data not shown), exactly as observed in vivo. Thus, CecA utilizes posttranslational translocation to enter the microsome lumen even when the cotranslational pathway is available. The N-RRL system therefore recapitulates our in vivo observations in an efficient in vitro system amenable to mechanistic manipulation.

Mapping Small-Protein Interactions during Posttranslational Translocation

To define the main steps of small-protein translocation, we combined temporal staging of the translocation reaction with general and site-specific crosslinking. In the cytosol, chemical crosslinking in N-RRL had revealed that CecA precursor associated almost exclusively with a ~20 kD protein (p20) (Figure 2C). Upon addition of RMs, the p20 interaction was lost concomitant with substrate translocation (Figure 3A). CecA crosslinking after translocation revealed a major ~60 kD partner (Figure 3A) that fractionated with RMs in sedimentation assays (Figure 3B). This crosslink was not observed when reconstituted RMs lacking lumenal proteins (LD-RMs) were used (Figure 3C), suggesting that p60 is a lumenal chaperone. We tested several candidates in immunoprecipitation experiments and found p60 to be PDI (Figure 3D). Photo-crosslinking with single probes incorporated into CecA confirmed that the PDI interaction is direct and selective to the mature domain (data not shown).

Translocation assays using LD-RMs resulted in signal-cleavage but not protease protection of CecA (Figure 3E). Similar results were obtained when high pH extraction was used to remove lumenal proteins (data not shown). In addition, while signal-cleaved CecA normally cosediments with intact RMs, signal-cleaved CecA produced with LD-RMs was cytosolic (data not shown). This suggests that in addition to interacting with translocated CecA, lumenal proteins are functionally necessary to complete CecA translocation into the ER lumen. This is similar to other translocation systems where lumenal proteins are thought to bias substrate transport at a late stage of translocation (Brodsky and Schekman, 1993; Nicchitta and Blobel, 1993; Panzner et al., 1995).

Thus, a cytosolic p20 interaction is converted to a PDI interaction in the ER lumen, presumably separated by the decisive translocation step across the membrane. This suggests that the mammalian small-protein translocation pathway might be conceptually analogous to posttranslational translocation in yeast, where translocation through the Sec61 channel is flanked by interactions with cytosolic and lumenal chaperones. It is therefore possible that CecA translocation could also involve the Sec61 complex given its high conservation (Rapoport, 2007). Consistent with this idea, we observed partial inhibition of CecA translocation with either a Sec61 inhibitor or competition with ribosomes translating a cotranslational Sec61 substrate

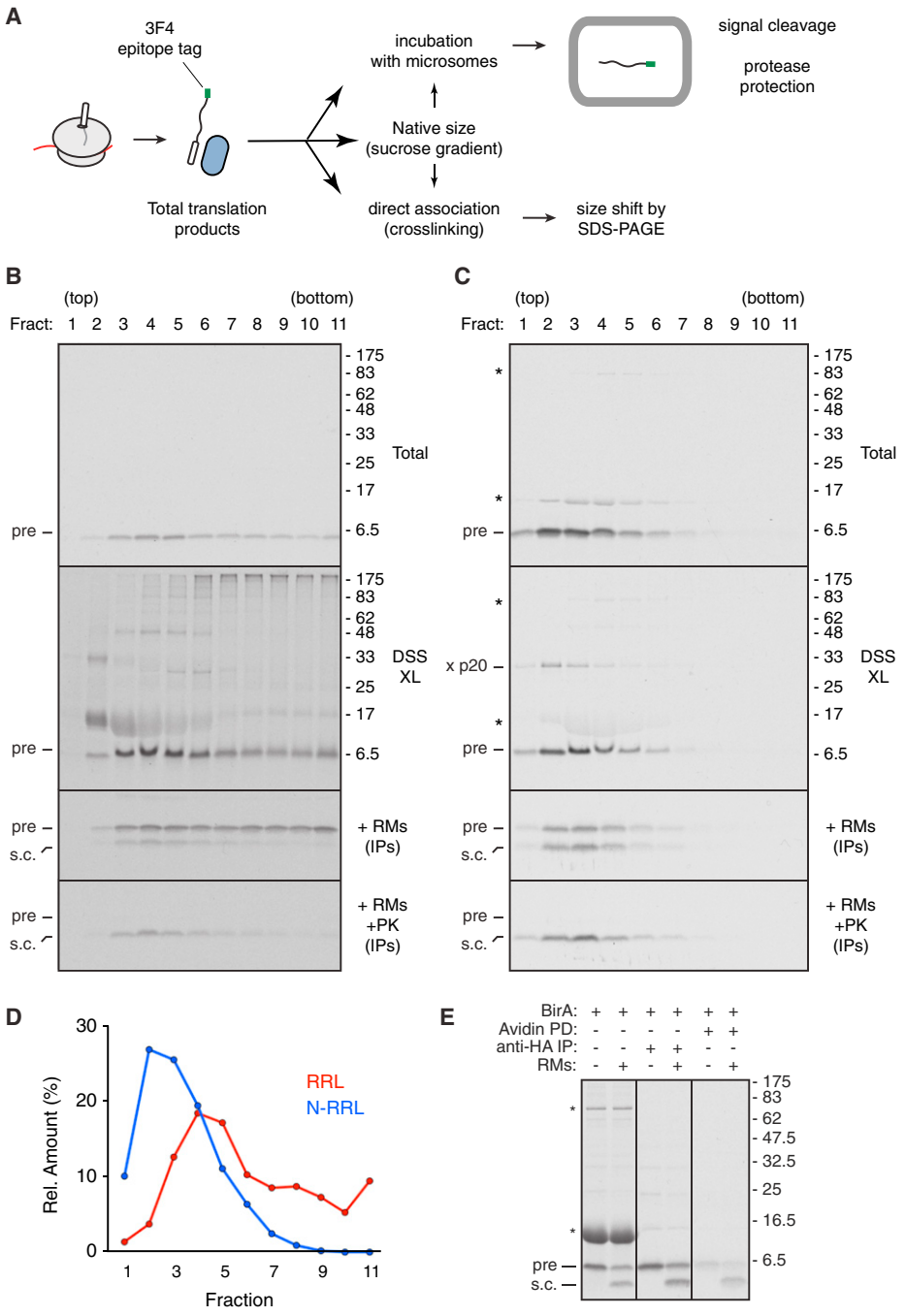

Figure 2. In Vitro Reconstitution of Small-Protein Posttranslational Translocation

(A) Schematic diagram of translocation and crosslinking assays used in this study.

(B and C) CecA tagged with a 3F4 epitope was translated in either conventional nuclease treated RRL (B) or nonnucleased "native" RRL (N-RRL) (C) and separated into 11 fractions on a 5%–25% sucrose gradient. Each fraction was analyzed directly (Total), after amine-reactive chemical crosslinking (DSS XL), incubated with rough microsomes (RMs), and/or treated with proteinase K (PK) as indicated. Some samples were subject to immunopreciptation (IP) before analysis. The positions of precursor and signal-cleaved products are shown. A prominent crosslink to a ~20 kD protein observed in N-RRL is indicated (x p20). Asterisks indicate background bands resulting from translation of endogenous mRNAs in N-RRL.

(D) Profiles of CecA migration on 5%–25% sucrose gradients when analyzed from RRL (red) versus N-RRL (blue).

(E) CecA was translated in BirA-containing N-RRL in the absence or presence of RMs. The samples were either analyzed directly, or after anti-HA IP or avidin PD as indicated. Note that signal-cleaved CecA is biotinylated, indicating its posttranslational translocation. The reduced recovery in the avidin PD samples is due to competing free biotin in the N-RRL.

See also Figure S2.

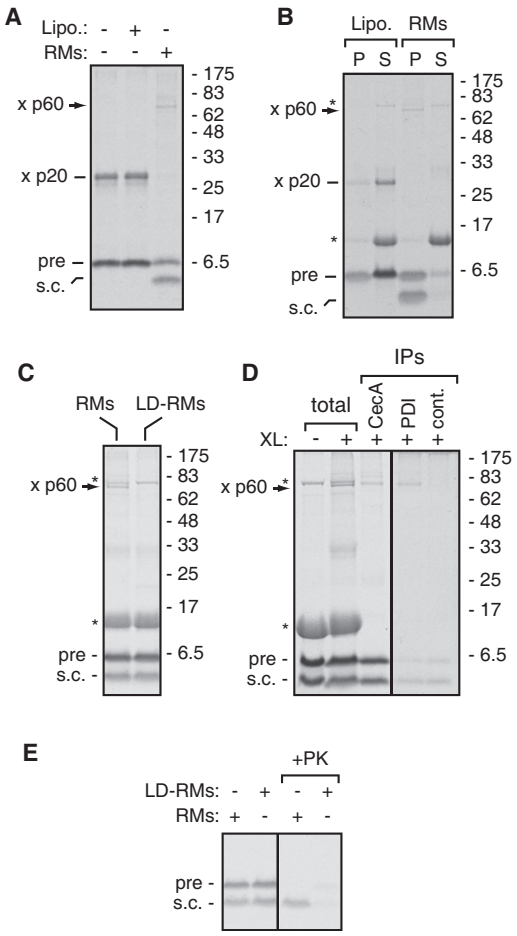

Figure 3. Analysis of Small-Protein Interactions at Different Stages of Translocation

(A) Crosslinking reactions (using the amine-reactive agent DSS) of CecA translations after incubation with buffer, liposomes, or RMs. The major crosslinks to p20 in the cytosol and p60 in the membrane are indicated. All samples are immunoprecipitations with anti-3F4 to recover CecA.

(B) Crosslinking reactions of CecA after incubation with either liposomes or RMs as in panel A were subjected to centrifugation to separate the vesicle pellet (P) from cytosolic supernatant (S). Note that the p20 crosslink is cytosolic, while p60 is in the membrane fraction. Asterisks are endogenous reticulocyte proteins.

(C) CecA translations were incubated with either RMs or LD-RMs (RMs depleted of lumenal proteins), and subjected to crosslinking.

(D) CecA crosslinking reactions were subjected to IPs with antibodies against the substrate (CecA), PDI, or an irrelevant antibody (cont.).

(E) CecA translocation reactions with either RMs or LD-RMs were analyzed by a protease protection assay.

(unpublished results). Future studies will be needed to investigate this possibility and rigorously analyze the membrane and lumenal steps in the CecA pathway. For the remainder of this study, we focus on the poorly characterized p20-substrate complex.

Identification of p20 as Calmodulin

In addition to CecA, p20 was the major crosslinking partner of other short secretory proteins, but not of longer secretory proteins (Figure S2 and data not shown). Furthermore, this interaction was lost upon translocation into RMs and was signal sequence specific since mutating hydrophobic residues in the CecA signal to charged residues prevented p20 association (Figure 4A). Importantly, the p20 interaction with CecA was observed to be equally efficient even when CecA was translated at ~10-fold lower levels (data not shown). This illustrated that p20 was not a 'secondary' interaction partner seen only after saturating another factor. Thus, for multiple short proteins, p20 is a major and transient signal sequence-dependent interaction partner in the cytosol.

Affinity purification of CecA precursor from large-scale translation reactions copurified p20 in a signal-dependent manner, and mass mapping subsequently identified p20 to be calmodulin (CaM) (Figure 4B). Immunoblotting of affinity-purified CecA and immunoprecipitation of CecA crosslinking reactions confirmed that CaM is the primary signal sequence-specific interacting partner in the cytosol (Figures 4B and 4C). CaM is an abundant, ubiquitously expressed, and highly conserved protein capable of binding short ~7–15 residue peptides of tremendous sequence diversity (O'Neil and DeGrado, 1990). This promiscuity of CaM is facilitated by a substrate-binding site rich in methionine residues, whose hydrophobic flexible side chains can accommodate widely variable hydrophobic targets. A similar methionine-rich binding pocket is seen in the signal sequence binding domain of SRP (Figures S3A–S3C) (Keenan et al., 1998) and the transmembrane domain binding region of Get3 (Mateja et al., 2009). This suggested that CaM can bind directly to the signal sequences of small proteins, a hypothesis validated by site-specific photo-crosslinking experiments (Figure 4D). Indeed, CaM was previously observed to bind isolated signal sequences or fragments (Martoglio et al., 1997), although the relevance of this finding was not clear. Thus, CaM would appear to be a major signal sequence binding protein for small secretory proteins released into the cytosol.

CaM Requires Physiologic [Ca^{2+}] for Signal Sequence Interaction

Why did our initial crosslinking experiments in RRL fail to reveal CaM interactions? The answer proved to be inhibition of CaM binding to small-protein substrates by exogenously added EGTA. RRL translation systems are typically treated with a Ca^{2+}-dependent nuclease to remove endogenous mRNAs, followed by addition of 2 mM EGTA to inactivate the nuclease (Pelham and Jackson, 1976). This chelates free Ca^{2+}, which has four binding sites on CaM, and influences its ability to bind many of its substrates. By contrast, the nonnuclease N-RRL system lacks EGTA, and therefore contains endogenously derived cytosolic Ca^{2+}. This suggested that the key feature of N-RRL was the absence of EGTA. Indeed, standard RRL can be 'rescued' in its activity by fractionation to remove the nuclease and EGTA (Figure S3D). Like N-RRL (Figure 2C), this fractionated RRL (Fr-RRL) shows homogeneous substrate complexes, efficient CaM interaction, and improved CecA translocation (Figure S3E). Addition of EGTA (independent of nuclease) to either N-RRL or Fr-RRL (Figure 4E and data not shown) inhibited substrate interaction with CaM and decreased translocation efficiency (Figure 4F). Similar results were seen for

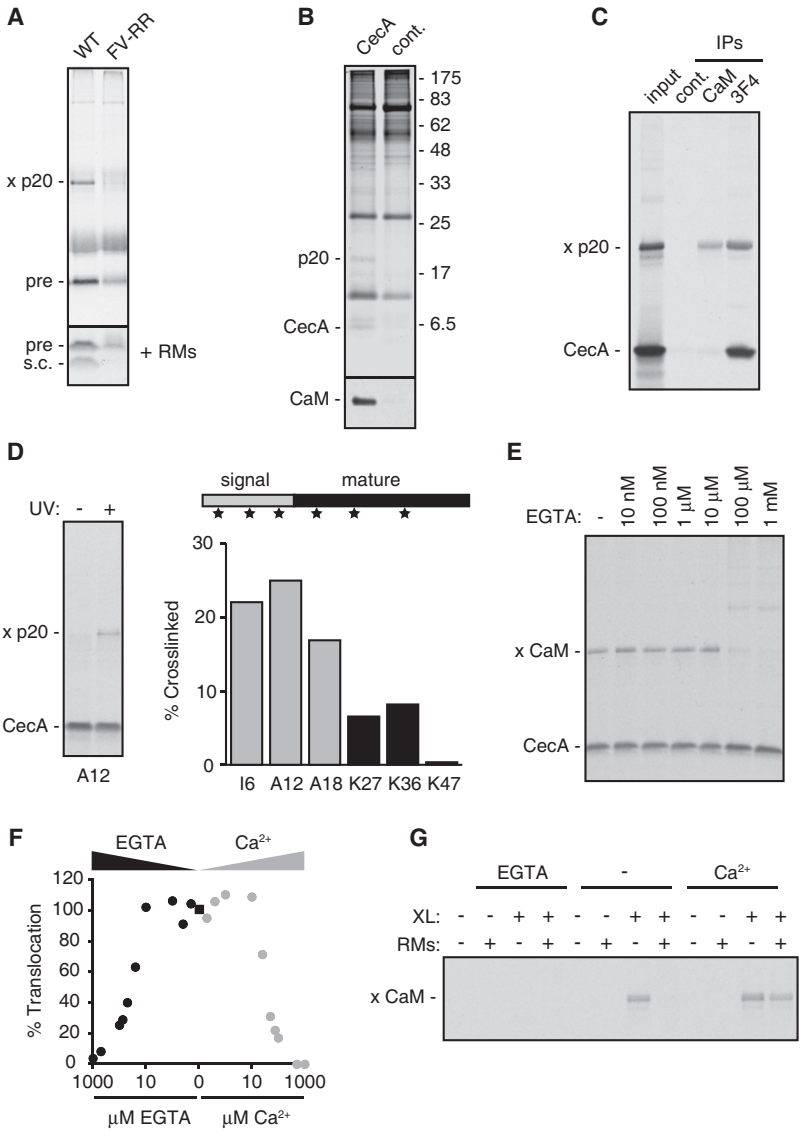

Figure 4. Calmodulin Interacts with Small-Protein Signal Sequences

(A) Two hydrophobic residues in the CecA signal sequence were mutated to argininies (FV-RR) and tested for interaction with p20 by crosslinking in N-RRL. The bottom panel shows the results of translocation assays using RMs.

(B) Large-scale translations of CecA or a control reaction were affinity purified via the 3F4 tag on CecA and analyzed by coomassie blue staining (top) or immunoblotting with anti-calmodulin (CaM). The p20 band was identified as CaM by mass spectrometry.

(C) CecA crosslinking reaction was analyzed directly (input) or after IP with the indicated antibodies. 3F4 recognizes the tag on CecA, while "cont." indicates irrelevant antibody.

(D) Single photo-crosslinking probes were introduced into different positions of CecA by amber suppression and subjected to UV irradiation to detect p20 interactions. The relative crosslinking efficiencies at each position are plotted, with one example shown on the left.

(E) CecA was translated in the presence of the indicated concentrations of EGTA and subjected to crosslinking.

(F) CecA was translated in N-RRL with various amounts of EGTA and Ca^{2+} and posttranslational translocation activity relative to untreated lysate (square) was quantified.

(G) CecA was translated without or with 0.5 mM EGTA or 0.5 mM Ca^{2+}, incubated without or with RMs, and subjected to crosslinking. The region of the gel showing the CecA-CaM crosslink is displayed.

See also Figure S3.

two other small proteins (data not shown). Thus, efficient posttranslational translocation and the CaM interaction were previously obscured from discovery by the long-standing practice of treating translation systems with a Ca^{2+}-activated nuclease.

Although the precise relationship between Ca^{2+} binding to the four potential sites of CaM and its activity in signal sequence recognition remains to be fully characterized, CaM interaction and translocation activity were robust at a range of Ca^{2+} concentrations that encompasses the physiologic cytosolic Ca^{2+} levels found in N-RRL. However, either Ca^{2+} chelation with > 10 µM EGTA or excess Ca^{2+} > 10 µM resulted in reduced CecA translocation (Figure 4F). Crosslinking analysis showed that with EGTA, CaM is unable to interact with translocation substrates, whereas excessively high Ca^{2+} concentrations preclude efficient CaM release from translocation substrates when RMs were added (Figure 4G). These experiments illustrate that unlike a canonical CaM interaction that is only induced upon Ca^{2+} influx into the cytosol, CaM binding and release from signal sequences is fully operational at basal cytosolic Ca^{2+} concentration. Such a 'constitutive' activity was important in postulating a physiologic role in translocation, since our in vivo studies were performed under normal conditions where cytosolic [Ca^{2+}] would be ~10–100 nM (Carafoli, 1987). Thus, although CaM would seem to be an unlikely component of a constitutive cellular pathway, its ability to operate at widely ranging [Ca^{2+}], signal sequence selectivity, ubiquity, abundance, and flexible nature of its hydrophobic binding site all support a direct functional role in posttranslational translocation.

Calmodulin Is Required for Efficient Posttranslational Translocation

To directly test this, we selectively depleted CaM from N-RRL by passing the lysate over a resin of immobilized CaM binding peptide (Means et al., 1991; Figure 5A). Depletion was better than 90% as judged by both immunoblotting and undetectable CaM-CecA crosslinks (Figures 5A and 5B). Relative to mock-depleted lysate, CaM-depleted lysates were selectively diminished in posttranslational CecA translocation with no discernable effect on cotranslational Prl translocation (Figures 5C and 5D). This deficiency was fully rescued by adding back physiologic levels of recombinant CaM, which interacted effectively with small substrates (Figure 5B). Importantly, the levels of other

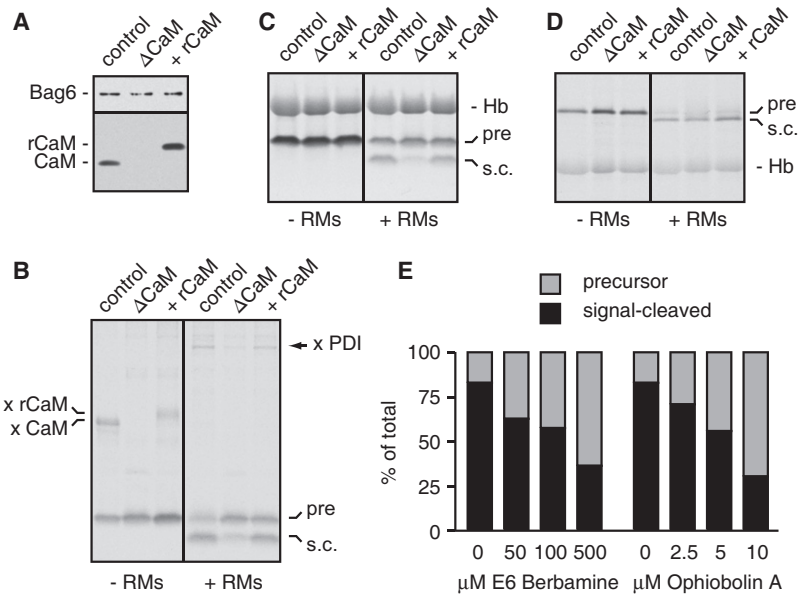

Figure 5. Calmodulin Is Required for Efficient Small-Protein Translocation

(A) N-RRL was passed over a GST resin (control) or GST-calmodulin binding peptide (CBP) resin (ΔCaM). The ΔCaM lysate was complemented with HA-tagged recombinant CaM (rCaM) purified from *E. coli*. Immunoblots for CaM and Bag6 (a control protein) are shown.

(B) CaM depletion specifically impairs CecA interaction with CaM by crosslinking (left panel). After incubation with RMs, CecA produced in the absence of CaM does not crosslink with PDI (right panel). Both effects are rescued by rCaM.

(C) Posttranslational translocation of CecA is impaired by CaM depletion and restored by rCaM. Hb is endogenous hemoglobin.

(D) CaM depletion does not affect Prl cotranslational translocation.

(E) HeLa cells expressing CecA were pulse labeled without or with CaM inhibitors, and the relative proportions of precursor and signal-cleaved forms of CecA quantified.

See also Figure S4.

cytosolic chaperones, such as Hsp70, were unchanged after CaM depletion (data not shown). Furthermore, CecA translocation was reduced in CaM depleted lysates even when RMs were included cotranslationally (Figure S4A), showing that neither cytosolic chaperones nor the cotranslational pathway can fully replace CaM's role.

To examine the importance of CaM in vivo, we used two independent membrane-permeable CaM inhibitors, E6 Berbamine and Ophiobolin A. In vitro studies verified that both inhibit CaM binding to CecA (data not shown). When applied to HeLa cells, both inhibitors reduced CecA translocation as judged by the relative ratio of precursor to signal-cleaved forms recovered from pulse-labeled cells (Figure 5E). As expected, neither inhibitor had an effect on Prl translocation (Figure S4B). Because the inhibitors were applied acutely during the labeling period, potential indirect effects were minimized. Thus, CecA apparently cannot effectively utilize either the SRP-dependent cotranslational pathway or other chaperones when CaM is inhibited in vivo. This suggests that a substantial proportion of CecA follows the CaM-dependent posttranslational pathway.

Calmodulin Maintains Translocation Competence of Small Proteins

To understand the mechanism by which CaM facilitates posttranslational translocation, we analyzed substrate fate in the presence and absence of CaM. We found that for several small secretory proteins, CaM's role was to prevent their heterogeneous engagement into various high molecular weight complexes, including possible aggregation (Figure 6A). This was observed not only with EGTA (e.g., Figure 2 and Figure S2), but also with selective CaM depletion (Figure 6A). In addition, small proteins bound to CaM retained their translocation competence over the course of an hour, but lost competence rapidly after CaM dissociation with EGTA (Figure 6B). This loss of translocation competence was largely irreversible since subsequent restoration of Ca^{2+} could not effectively rescue CecA translocation (Figure 6C). Instead, substrates forcibly dissociated from CaM made various off-pathway interactions as detected by crosslinking. Among these interactions, one binding partner was Bag6 (data not shown), a hydrophobic domain binding protein that was recently shown to be a quality control factor for degrading mislocalized proteins (Hessa et al., 2011). Indeed, small-protein precursors are more extensively ubiquitinated in the absence compared to presence of CaM activity (Figure 6D). Thus, CaM binding to short secretory proteins protects their hydrophobic signal sequences from terminal off-pathway fates, thereby maintaining their solubility and translocation competence.

Calmodulin Dissociation Is Rate Limiting for Translocation

Since CaM does not accompany its substrate into the ER lumen, it must release substrate for translocation to occur. A key issue is how this release is effected. One possibility is that CaM-substrate interactions are dynamic and that the unbound population of substrate is able to engage the translocation machinery. Alternatively, release might be mediated by a putative receptor on the RMs, with CaM therefore playing the role of a specific targeting factor. Indeed, CaM was recently found to interact with Sec61α (Erdmann et al., 2011), which would provide an attractive targeting mechanism for small-protein substrates. To discriminate between these models, we analyzed the nature of CaM-substrate interaction dynamics.

We found that in the cytosol (without RMs), the CecA-CaM complex was dynamic. This was illustrated by the finding that addition of recombinant GST-CaM to pre-formed CecA-CaM complexes results in CecA equilibration between the endogenous and recombinant CaM (Figure 7A). A time course using photo-crosslinking showed that transfer from CaM to GST-CaM began within five minutes and equilibrated with a time

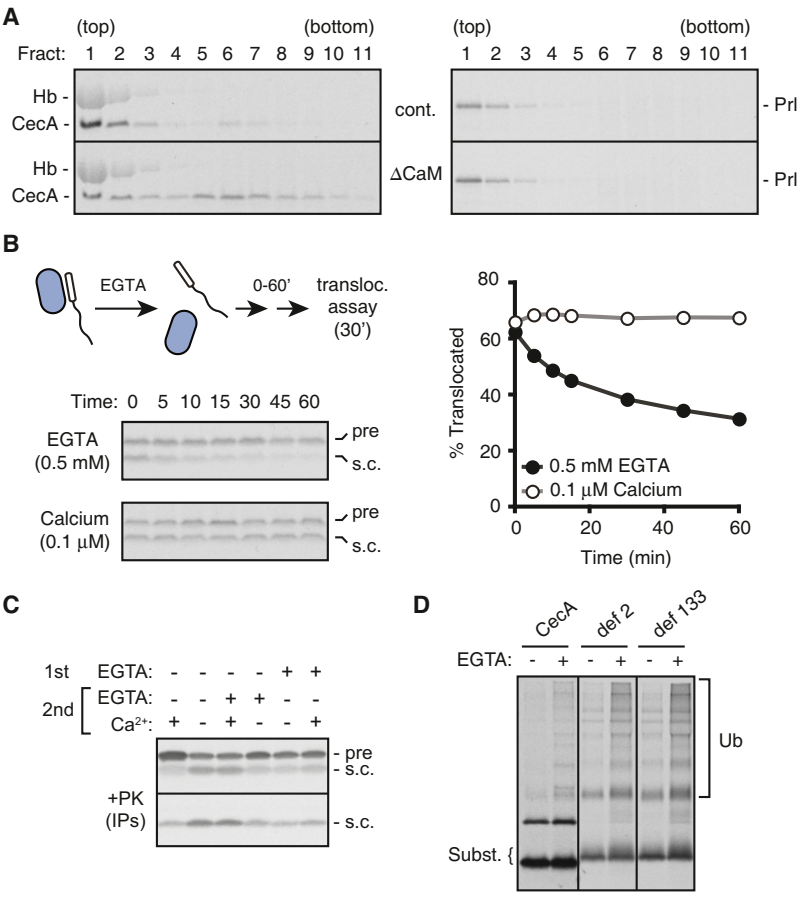

Figure 6. Calmodulin Maintains Translocation Competence of Small Proteins

(A) Fractions from a 10%–50% sucrose gradient separation of CecA (left panels) or Prl (right panels) translated in N-RRL not depleted or depleted of CaM. CecA engages in high molecular weight complexes in the absence of CaM, while endogenous Hemoglobin (Hb) and Prl are unaffected.

(B) CecA-CaM complexes made in N-RRL were dissociated with 0.5 mM EGTA or preserved with 0.1 μM Ca^{2+} and after various times at 32°C, tested for translocation into RMs. The quantified results from the gel are shown in the graph.

(C) CecA translated in N-RRL was posttranslationally subjected to two successive treatments. First, samples were incubated without or with 0.5 mM EGTA to disrupt CaM-CecA complexes for 15 min at 32°C (1st). Second, samples were incubated for another 15 min without or with 0.5 mM Ca^{2+}, 0.5 mM EGTA, or both (2nd). RMs were then added to assay for translocation by either signal cleavage (top panel) or protease protection (bottom).

(D) CecA, defensin 2, and defensin 133 were each translated in N-RRL without or with 0.5 mM EGTA. The high molecular weight ladder seen with EGTA was confirmed to represent ubiquitinated species (data not shown).

course that closely matched the time course for posttranslational translocation (Figure 7B). This suggested that the intrinsic rate of release from CaM may be the rate-limiting event for posttranslational translocation. To test this, we asked what would happen if substrate release from CaM were prematurely induced. In the spontaneous release model, this should increase the rate of substrate translocation. By contrast, a receptor-mediated model would predict decreased translocation since the substrate would no longer be bound to its targeting factor.

CaM-CecA complexes were dissociated with EGTA in the presence of RMs and the extent of translocation at multiple time points was assessed (Figure 7C). A clear acceleration of rate was observed under these conditions, with translocation being nearly complete within 5 min. Note that the converse is also true: slowing down substrate release from CaM by increased Ca^{2+} levels leads to reduced translocation (Figure 4F and 4G). Thus, at least under the conditions of this N-RRL in vitro system, CaM binding to substrates is dynamic, and the rate-limiting step in translocation is determined by the kinetics of substrate release. While a receptor does not seem to be obligatory, it could nonetheless improve efficiency or reduce off-pathway reactions by favoring substrate release close to its site of translocation. This remains to be investigated, particularly the intriguing interaction between Sec61α and CaM (Erdmann et al., 2011).

Conclusions and Perspective

While short secreted proteins were once considered unusual, they are now appreciated to serve a wide range of functions in metazoans. Notable examples include antimicrobial peptides essential for innate immunity, various toxins, hormones, chemokines, and others whose precursors are encoded by short open reading frames (Brogden, 2005; Schluger and Rom, 1997; Table S1). In addition, recent ribosome profiling analyses (Ingolia et al., 2009) and bioinformatic studies (Frith et al., 2006) indicate that many short proteins remain unannotated and that a significant portion of these may contain hydrophobic signal sequences for targeting to the secretory pathway. Our results provide new mechanistic insights into how small secretory proteins enter the mammalian ER.

We have illustrated both in vitro and in vivo that short proteins utilize a posttranslational translocation pathway and identify CaM as a specific chaperone that stabilizes the cytosolic intermediate in this process (Figure 7D). CaM directly binds to the hydrophobic signal sequences of short secretory proteins in a Ca^{2+}-regulated manner, shielding them from detrimental fates in the aqueous cytosol, preventing their recognition by quality control, and maintaining their ability to translocate. This pathway fills a niche that cannot be fully accommodated by either the SRP-dependent cotranslational pathway or general cytosolic chaperones. Hence, even under cotranslational translocation conditions in vitro or in vivo, a substantial amount of translocated CecA was derived from a cytosolic intermediate. Furthermore, selective depletion or inhibition of CaM substantially reduced small-protein translocation and increased off-pathway fates. Thus, CaM-dependent translocation is a major (but perhaps not exclusive) pathway used by small proteins.

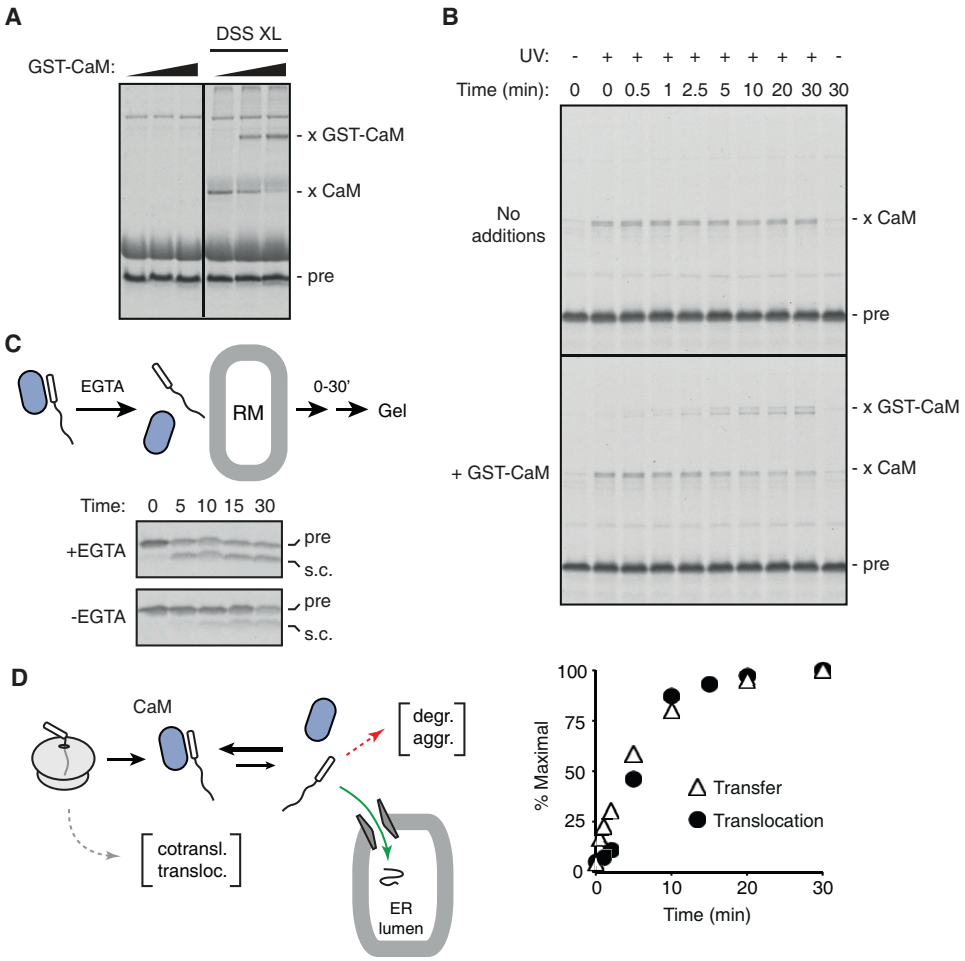

Figure 7. Calmodulin Release Is Rate Limiting for Small-Protein Translocation

(A) CecA translated in N-RRL was posttranslationally incubated without or with different concentrations of recombinant GST-CaM for 30 min at 32°C and subjected to crosslinking (DSS XL). The positions of crosslinks to CaM and GST-CaM are indicated.

(B) CecA containing a photo-crosslinking probe at residue 12 translated in Fr-RRL was posttranslationally incubated without (top) or with (bottom) GST-CaM at levels equimolar to endogenous CaM. After incubation for the indicated times at 32°C, the samples were rapidly flash frozen in liquid nitrogen and crosslinked on dry ice with UV light. Controls without UV at the extreme time points are also shown. The extent of transfer to GST-CaM (normalized to the 30 min time point) is plotted relative to CecA translocation assayed under similar conditions (also normalized to the 30 min time point).

(C) CecA-CaM complexes made in N-RRL were dissociated with 0.5 mM EGTA in the presence of RMs, incubated for varying times, and analyzed by SDS-PAGE. Translocation occurs within 5 min after EGTA dissociation but is normally slower at endogenous Ca^{2+} levels.

(D) Working model. Small proteins have poor access to cotranslational translocation, but instead interact dynamically with CaM in the cytosol. This prevents degradation and aggregation, while still allowing translocation to occur upon CaM release. See Table S1 for examples of small secretory proteins that may use this pathway.

The observation that CaM depletion (or inhibition) could not be readily compensated by other abundant polypeptide binding proteins was unexpected. This differs from yeast, where multiple chaperones, most notably of the Hsp70 family, interact with and maintain translocation competence of substrates. The mammalian orthologs of these chaperones are clearly functional since a yeast substrate (prepro-α-factor) synthesized in nuclease RRL can interact with them and posttranslationally translocate into yeast RMs (Plath and Rapoport, 2000; Rothblatt et al., 1987). So why are the mammalian orthologs of these chaperones unable to fulfill the same function for small proteins? One reason might be the need for more complete shielding of the hydrophobic signal sequence to prevent aggregation. Indeed, substrates engage in large translocation-incompetent complexes in the absence of CaM, despite the availability of the full complement of cytosolic chaperones. This might not be a problem in yeast where posttranslational substrates typically have signal sequences of lower hydrophobicity (Ng et al., 1996), and any aggregation can be reversed by Hsp104, a fungal specific chaperone (Doyle and Wickner, 2009).

In addition, metazoans often couple their chaperone systems more directly to ubiquitination pathways (Hessa et al., 2011; McConough and Patterson, 2003). Hence, CaM can maintain its substrates in a translocation competent state without the

risk of rapid degradation. Consistent with this idea, small-protein substrates are ubiquitinated in vitro in the absence of CaM, and CaM-independent precursors (but not CaM-dependent ones) are rapidly degraded in a proteasome-dependent pathway in vivo. Thus, while general cytosolic chaperones can maintain translocation competence of small proteins in principle, CaM's signal sequence selectivity, ability to completely wrap around and shield its substrate, and lack of coupling to ubiquitination machinery all afford advantages.

Finally, high volume secretion of small proteins, such as insulin and beta-defensin-2, are often accompanied by significant changes in intracellular Ca^{2+} levels that directly affect secretion in multiple ways including transcription, translation, and trafficking (German et al., 1990; Krisanaprakornkit et al., 2003; Pernet et al., 2003). This imposes rapid and very large changes in translocation load without sufficient time to increase translocon abundance. It is attractive to speculate that the ability of CaM to efficiently maintain translocation competence, particularly under high Ca^{2+} conditions, may buffer against temporary increases in small-protein production without having to degrade the excess. Given that CaM is the target of much regulation, one might also anticipate that small-protein secretion could be responsive to changing needs and extracellular cues.

EXPERIMENTAL PROCEDURES

Reagents and Standard Methods

All plasmid constructs have been described or are minor modifications to existing constructs produced using standard methods (Stefanovic and Hegde, 2007; Emerman et al., 2010). CaM antibody was obtained from Abcam. All other antibodies, in vitro translations and biotinylation, sucrose gradients, chemical crosslinking, photocrosslinking, immunoblotting, affinity purification, immunoprecipitations, and avidin pulldowns have been described (Stefanovic and Hegde, 2007; Emerman et al., 2010; Hessa et al., 2011; Fons et al., 2003; Do et al., 32). Culture, transfection, and pulse-chase analysis of HeLa and 293T were as before (Emerman et al., 2010). Recombinant His-tagged and GST-tagged CaM, His-tagged BirA, and GST-tagged CaM binding peptide were purified from *E. coli* using standard procedures. Details are provided in the Extended Experimental Procedures of the Supplemental Information.

In Vivo Biotinylation

HeLa or HEK293T cells seeded in 6-well dishes were cotransfected with plasmids encoding substrate and BirA in a 4:1 ratio using Lipofectamine 2000 (Invitrogen). 16 hr after transfection, cells were radiolabeled with 150 μCi translabel for 1 hr (Emerman et al., 2010), harvested in 1% SDS, 0.1 M Tris, pH 8 and immediately boiled to fully solubilize all proteins and destroy all enzymatic activities. Pulldowns and immunoprecipitations were performed as described (Emerman et al., 2010) on samples diluted 10-fold in ice cold IP buffer (1% Triton X-100, 50 mM HEPES, (pH 7.4), 100 mM NaCl). For proteasome inhibition and CaM inhibition, 10 μM MG132 and/or inhibitors were added during labeling.

Translation Extracts

Fr-RRL has been described (Hessa et al., 2011; see Extended Experimental Procedures). N-RRL was made by reconstituting native RRL that had not been treated with hemin or nuclease into a translation system using the same final concentrations of components as the RRL and Fr-RRL translation systems (Hessa et al., 2011). CaM-depleted translation extract was produced by passing native RRL over GST-tagged CaM binding peptide immobilized on a glutathione sepharose column and reconstituting the flow-through into a translation system. Detailed protocols are provided in Extended Experimental Procedures.

In Vitro Translation and Translocation

In vitro transcription and translation in RRL and Fr-RRL in the presence of ^{35}S-methionine were as described before for 30 min at 32°C (Stefanovic and Hegde, 2007; Hessa et al., 2011; Sharma et al., 2010). Translation in N-RRL was the same as in RRL except that the translation extract was made with a completely 'native' RRL (i.e., nonnucleased and nonhemin treated). Final concentrations of all other additives remain the same. Thus, N-RRL contains the endogenous level of cytosolic Ca^{2+} derived from the reticulocyte cytosol, and any trace amounts contributed by the water and other shelf chemicals. Cotranslational translocation assays into RMs have been described previously (Fons et al., 2003). For posttranslational translocation assays, translation was terminated by either adding 10 μg/ml RNase A and/or by removing of ribosomes by ultracentrifugation (70,000 rpm in the TLA120.1 rotor (Beckman) for 30 min at 4°C). Translocation was initiated by adding RMs (derived from either canine or porcine pancreas; Walter and Blobel, 1983). The addition of recombinant proteins and calcium and EGTA manipulations were as described in the individual figure legends. Unless otherwise noted, translocation assays were for 30 min at 32°C, except for those shown in Figure 7C, which were conducted at 37°C. Protease protection assay for translocated products was as before (Stefanovic and Hegde, 2007; Fons et al., 2003). For immunoprecipitations or pulldowns, samples were first denatured by boiling to 100°C in 1% SDS, 0.1 M Tris, pH 8, then treated as described above for IPs or pulldowns from cultured cells. Translocation efficiencies were quantified with either Image J or by phosphorimaging using a Typhoon scanner. All band intensities were subtracted of background intensities and normalized for the number of methionines expected to be in the products.

Sucrose Gradients, Crosslinking, and Translocation

In most experiments, 200 μl translation reactions were layered on a 2 ml 5%–25% sucrose gradients in physiologic salt buffer (PSB: 50 mM Hepes, [pH 7.4], 100 mM KAc, 2 mM $MgAc_2$) and centrifuged for 5 hr at 55,000 rpm at 4°C in the TLS-55 rotor (Beckman). Eleven 200 μl fractions were then removed from the top. For translocation assays of sucrose gradient fractions, RMs were added (composing one tenth of the reaction volume), the reaction supplemented with an energy-regenerating system (1 mM ATP, 1 mM GTP, 10 mM Creatine phosphate, 40 μg/ml Creatine Kinase) and 1 mM DTT, and incubated for 30 min at 32°C. The remaining analysis was as above. Chemical crosslinking experiments of sucrose gradient fractions were performed with 250 μM DSS at room temperature for 30 min, quenched with 100 mM Tris, and samples were then subject to direct analysis or immunoprecipitation. For crosslinking of RRL, or N-RRL translation reactions, the samples were first diluted 10-fold in PSB (to dilute primary amines) before adding crosslinker as above. Fr-RRL was crosslinked directly since its buffer composition was known (see above) to lack primary amines. Photocrosslinking using benzophenone-modified or 4,4-azipentanoyl-modified lysyl-tRNA (from tRNA Probes) was as before (Do et al., 1996; Krieg et al., 1986), except Fr-RRL was used for the translation and the suppressor tRNA was included in the translation reaction at a final concentration of 1 μM. Both probes gave similar site-specific and crosslinking efficiency results. Crosslinking time courses were performed by rapidly freezing samples in liquid nitrogen at the indicated time points and UV irradiating on dry ice (Plath et al., 2004). Size fractionation of CecA and Prl in CaM-depleted lysates were on a 10%–50% sucrose gradient in PSB centrifuged at 55,000 rpm for 1 hr at 4°C in the TLS-55 rotor, after which 200 μl fractions were collected and analyzed directly.

SUPPLEMENTAL INFORMATION

Supplemental Information includes Extended Experimental Procedures, one table, and four figures and can be found with this article online at doi:10.1016/j.cell.2011.11.048.

ACKNOWLEDGMENTS

We are grateful to M. Mariappan for useful discussions; S. Appathurai for initial experiments and reagents; A. Sharma for technical help; other Hegde lab members for support; and K. Strub for sharing results prior to publication.

This work was supported by the JHU-NIH Graduate Partnership Program, the Intramural Research Program of the NICHD, and the Medical Research Council.

Received: July 26, 2011
Revised: September 15, 2011
Accepted: November 22, 2011
Published: December 22, 2011

REFERENCES

Brodsky, J.L., and Schekman, R. (1993). A Sec63-BiP complex from yeast is required for protein translocation in a reconstituted proteoliposome. J. Cell Biol. *123*, 1355–1363.

Brogden, K.A. (2005). Antimicrobial peptides: pore formers or metabolic inhibitors in bacteria? Nat. Rev. Microbiol. *3*, 238–250.

Carafoli, E. (1987). Intracellular Calcium Homeostasis. Annu. Rev. Biochem. *56*, 395–433.

Chirico, W.J., Waters, M.G., and Blobel, G. (1988). 70K heat shock related proteins stimulate protein translocation into microsomes. Nature *332*, 805–810.

Deshaies, R.J., Koch, B.D., Werner-Washburne, M., Craig, E.A., and Schekman, R. (1988). A subfamily of stress proteins facilitates translocation of secretory and mitochondrial precursor polypeptides. Nature *332*, 800–805.

Deshaies, R.J., Sanders, S.L., Feldhelm, D.A., and Schekman, R. (1991). Assembly of yeast Sec protein involved in translocation into the endoplasmic reticulum into a membrane-bound multisubunit complex. Nature *349*, 806–808.

Do, H., Falcone, D., Lin, J., Andrews, D.W., and Johnson, A.E. (1996). The cotranslational integration of membrane proteins into the phospholipid bilayer is a multistep process. Cell *85*, 369–378.

Doyle, S.M., and Wickner, S. (2009). Hsp104 and ClpB: protein disaggregating machines. Trends Biochem. Sci. *34*, 40–48.

Emerman, A.B., Zhang, Z.-R., Chakrabarti, O., and Hegde, R.S. (2010). Compartment-restricted biotinylation reveals novel features of prion protein metabolism in vivo. Mol. Biol. Cell *21*, 4325–4337.

Erdmann, F., Schäuble, N., Lang, S., Jung, M., Honigmann, A., Ahmad, M., Dudek, J., Benedix, J., Harsman, A., Kopp, A., et al. (2011). Interaction of calmodulin with Sec61α limits Ca^{2+} leakage from the endoplasmic reticulum. EMBO J. *30*, 17–31.

Frith, M.C., Forrest, A.R., Nourbakhsh, E., Pang, K.C., Kai, C., Kawai, J., Carninci, P., Hayashizaki, Y., Bailey, T.L., and Grimmond, S.M. (2006). The abundance of short proteins in the mammalian proteome. PLoS Genet. *2*, e52.

Fons, R.D., Bogert, B.A., and Hegde, R.S. (2003). Substrate-specific function of the translocon-associated protein complex during translocation across the ER membrane. J. Cell Biol. *160*, 529–539.

Garcia, P.D., and Walter, P. (1988). Full-length prepro-α-factor can be translocated across the mammalian microsomal membrane only if translation has not terminated. J. Cell Biol. *106*, 1043–1048.

German, M.S., Moss, L.G., and Rutter, W.J. (1990). Regulation of insulin gene expression by glucose and calcium in transfected primary islet cultures. J. Biol. Chem. *265*, 22063–22066.

Goder, V., Crottet, P., and Spiess, M. (2000). In vivo kinetics of protein targeting to the endoplasmic reticulum determined by site-specific phosphorylation. EMBO J. *19*, 6704–6712.

Hessa, T., Sharma, A., Mariappan, M., Eshleman, H.D., Gutierrez, E., and Hegde, R.S. (2011). Protein targeting and degradation pathways are coupled for elimination of mislocalized proteins. Nature, in press. 10.1038/nature10181.

Ingolia, N.T., Ghaemmaghami, S., Newman, J.R.S., and Weissman, J.S. (2009). Genome-wide analysis in vivo of translation with nucleotide resolution using ribosome profiling. Science *324*, 218–223.

Keenan, R.J., Freymann, D.M., Walter, P., and Stroud, R.M. (1998). Crystal structure of the signal sequence binding subunit of the signal recognition particle. Cell *94*, 181–191.

Krieg, U.C., Walter, P., and Johnson, A.E. (1986). Photocrosslinking of the signal sequence of nascent preprolactin to the 54-kilodalton polypeptide of the signal recognition particle. Proc. Natl. Acad. Sci. USA *83*, 8604–8608.

Krisanaprakornkit, S., Jotikasthira, D., and Dale, B.A. (2003). Intracellular calcium in signaling human β-defensin-2 expression in oral epithelial cells. J. Dent. Res. *82*, 877–882.

Martoglio, B., Graf, R., and Dobberstein, B. (1997). Signal peptide fragments of preprolactin and HIV-1 p-gp160 interact with calmodulin. EMBO J. *16*, 6636–6645.

Mateja, A., Szlachcic, A., Downing, M.E., Dobosz, M., Mariappan, M., Hegde, R.S., and Keenan, R.J. (2009). The structural basis of tail-anchored membrane protein recognition by Get3. Nature *461*, 361–366.

Matlack, K.E.S., Misselwitz, B., Plath, K., and Rapoport, T.A. (1999). BiP acts as a molecular ratchet during posttranslational transport of prepro-α-factor across the ER membrane. Cell *97*, 553–564.

McConough, H., and Patterson, C. (2003). CHIP: a link between the chaperone and proteasome systems. Cell Stress Chap. *8*, 303–308.

Means, A.R., Bafchi, I.C., Van Berkum, M.F.A., and Rassmussen, C.D. (1991). Calmodulin. In Cellular Calcium, A. Practical Approach, J.G. McCormack, and J.H. Cobbold, eds. (Oxford: IRL Press), pp. 205–245.

Ng, D.T.W., Brown, J.D., and Walter, P. (1996). Signal sequences specify the targeting route to the endoplasmic reticulum. J. Cell Biol. *134*, 269–278.

Nicchitta, C.V., and Blobel, G. (1993). Lumenal proteins of the mammalian endoplasmic reticulum are required to complete protein translocation. Cell *73*, 989–998.

O'Neil, K.T., and DeGrado, W.F. (1990). How calmodulin binds its targets: sequence independent recognition of amphiphilic α-helices. Trends Biochem. Sci. *15*, 59–64.

Osborne, A.R., Rapoport, T.A., and van den Berg, B. (2005). Protein translocation by the Sec61/SecY channel. Annu. Rev. Cell Dev. Biol. *21*, 529–550.

Panzner, S., Dreier, L., Hartmann, E., Kostka, S., and Rapoport, T.A. (1995a). Posttranslational protein transport in yeast reconstituted with a purified complex of Sec proteins and Kar2. Cell *81*, 561–570.

Panzner, S., Dreier, L., Hartmann, E., Kostka, S., and Rapoport, T.A. (1995b). Posttranslational protein transport into the endoplasmic reticulum. Cold Spring Harb. Symp. Quant. Biol. *60*, 31–40.

Pelham, H.R.B., and Jackson, R.J. (1976). An efficient mRNA-dependent translation system from reticulocyte lysates. Eur. J. Biochem. *67*, 247–256.

Pernet, I., Reymermier, C., Guezennec, A., Branka, J.E., Guesnet, J., Perrier, E., Dezutter-Dambuyant, C., Schmitt, D., and Viac, J. (2003). Calcium triggers β-defensin (hBD-2 and hBD-3) and chemokine macrophage inflammatory protein-3α (MIP-3α/CCL20) expression in monolayers of activated human keratinocytes. Exp. Dermatol. *12*, 755–760.

Plath, K., and Rapoport, T.A. (2000). Spontaneous release of cytosolic proteins from posttranslational substrates before their transport into the endoplasmic reticulum. J. Cell Biol. *151*, 167–178.

Plath, K., Wilkinson, B.M., Stirling, C.J., and Rapoport, T.A. (2004). Interactions between Sec complex and prepro-α-factor during posttranslational protein transport into the endoplasmic reticulum. Mol. Biol. Cell *15*, 1–10.

Rapoport, T.A. (2007). Protein translocation across the eukaryotic endoplasmic reticulum and bacterial plasma membranes. Nature *450*, 663–669.

Rothblatt, J.A., Webb, J.R., Ammerer, G., and Meyer, D.I. (1987). Secretion in yeast: structural features influencing the post-translational translocation of prepro-α-factor in vitro. EMBO J. *6*, 3455–3463.

Schlenstedt, G., and Zimmermann, R. (1987). Import of frog prepropeptide GLa into microsomes requires ATP but does not involve docking protein or ribosomes. EMBO J. *6*, 699–703.

Schlenstedt, G., Gudmundsson, G.H., Boman, H.G., and Zimmermann, R. (1990). A large presecretory protein translocates both cotranslationally, using signal recognition particle and ribosome, and post-translationally, without these ribonucleoparticles, when synthesized in the presence of mammalian microsomes. J. Biol. Chem. *265*, 13960–13968.

Schlenstedt, G., Gudmundsson, G.H., Boman, H.G., and Zimmermann, R. (1992). Structural requirements for transport of preprocecropinA and related presecretory proteins into mammalian microsomes. J. Biol. Chem. *267*, 24328–24332.

Schluger, N.W., and Rom, W.N. (1997). Early responses to infection: chemokines as mediators of inflammation. Curr. Opin. Immunol. *9*, 504–508.

Shan, S.-O., and Walter, P. (2005). Co-translational protein targeting by the signal recognition particle. FEBS Lett. *579*, 921–926.

Sharma, A., Mariappan, M., Appathurai, S., and Hegde, R.S. (2010). In vitro dissection of protein translocation into the mammalian endoplasmic reticulum. Methods Mol. Biol. *619*, 339–363.

Stefanovic, S., and Hegde, R.S. (2007). Identification of a targeting factor for posttranslational membrane protein insertion into the ER. Cell *128*, 1147–1159.

Walter, P., and Blobel, G. (1983). Preparation of microsomal membranes for cotranslational protein translocation. Methods Enzymol. *96*, 84–93.

Zimmermann, R., and Mollay, C. (1986). Import of honeybee prepromellitin into the endoplasmic reticulum. Requirements for membrane insertion, processing, and sequestration. J. Biol. Chem. *261*, 12889–12895.

Zimmermann, R., Zimmermann, M., Wiech, H., Schlenstedt, G., Müller, G., Morel, F., Klappa, P., Jung, C., and Cobet, W.W.E. (1990). Ribonucleoparticle-independent transport of proteins into mammalian microsomes. J. Bioenerg. Biomembr. *22*, 711–723.

EXTENDED EXPERIMENTAL PROCEDURES

Plasmids and Antibodies

Mammalian expression vectors for mCer-BirA (the *E. coli* biotin ligase tagged with monomeric Cerulean fluorescent protein for facile detection) and GFP (a control used in lieu of mCer-BirA) have been described previously (Emerman et al., 2010). SP64 vector-based constructs encoding CecA, defensin 2, defensin 133, and apamin were produced by annealing ultramer oligos (from IDT) encoding the cDNA of the small secretory proteins and subcloning them into the SP64 vector upstream of a C-terminal 3F4 epitope tag (KTNMKHMAGAAA). The SP64-vector based construct encoding Prl has been previously described (Fons et al., 2003). Prl-CecA and CecA-Prl were produced by introducing a BspEI site between the signal sequence and mature domain of CecA by site-directed mutagenesis followed by use of this site to replace either the signal or mature domain by standard methods. The BioTag-HA epitope was incorporated into Prl, CecA, Prl-CecA, and CecA-Prl using site-directed mutagenesis and then subcloned from the SP64 vector to a pcDNA-based vector for mammalian expression. It is worth noting that the epitope tags (3F4 or BioTag-HA) were engineered so as to maintain the overall short length of the protein well within the 100-residue limit. Thus, the BioTag-HA cassette replaced the same length of sequence at the end of the native protein, while appending the 3F4 tag increased overall length only modestly. The FV-RR signal sequence mutation in CecA replacing residues 9 and 10 with two arginines was made by site-directed mutagenesis. Individual amber mutations in CecA at residues 6, 12, 18, 27, 36, and 47 were produced by site-directed mutagenesis. For in vitro translations, the open reading frames were PCR amplified using a forward 5′ primer annealing to the SP6 promoter, and a reverse primer in the 3′ UTR at least 100 nucleotides beyond the stop codon (Sharma et al., 2010). His-tagged BirA was subcloned into the pRSET-A vector (which contains a His6 tag for purification) using standard methods for purification of the recombinant enzyme. The initial cDNA of CaM was purchased from Origene and subcloned with an additional HA tag into a pRSET-A vector or the GST-containing pGEX 6P-1 vector for bacterial expression of HA-CaM and GST-CaM, respectively. The calmodulin binding peptide coding sequence (CBP: KRRWKKNFIAVSAANRFKKISSSGAL) was subcloned into the pGEX 6P-1 vector for expression of a GST-CBP fusion protein. CaM antibody was purchased from Abcam. Antibodies to 3F4, HA, and Bag6 have been previously described (Stefanovic and Hegde, 2007; Ashok and Hegde, 2008; Mariappan et al., 2010).

In Vivo Biotinylation

Culture and transfection of HeLa and HEK293T cells have been described. With some modifications from a published procedure (Emerman et al., 2010), cells were seeded in 6-well dishes and cotransfected with plasmids encoding substrate and either mCer-BirA (labeled "+BirA" in the figures) or GFP (the "-BirA" control) in a 4:1 ratio using Lipofectamine 2000 (Invitrogen) according to the supplier's instructions. Fluorescence inspection confirmed at least 70% transfection efficiency. 16 hr after transfection, cells were starved for 30 min in media lacking cysteine and methionine supplemented with 10% dialyzed FBS, and then radiolabeled with 150 μCi translabel for 1 hr. Cells were harvested in 1% SDS, 0.1 M Tris, (pH 8), and immediately boiled to fully solubilize all proteins and destroy all enzymatic activities. The DNA was sheared by vigorous vortexing. Pulldowns and immunoprecipitations were performed as described (Emerman et al., 2010) on samples diluted 10-fold in ice cold IP buffer (1% Triton X-100, 50 mM HEPES, [pH 7.4], 100 mM NaCl). Any insoluble material was removed by centrifugation in a microcentrifuge, and the supernatant immunoprecipitated with anti-HA or anti-GFP (control) antibodies, or subject to pulldown by Avidin-agarose beads (Pierce). Total, immunoprecipitated, and avidin pulldown samples were analyzed by SDS-Page and autoradiography. For proteasome inhibition and CaM inhibition, 10 μM MG132 and/or inhibitors were added during starvation and labeling. E6 Berbamine and Ophiobolin A were purchased from Enzo Life Sciences and dissolved in DMSO. Subcellular fractionation with digitonin employed previously established methods (Levine et al., 2005). Briefly, radiolabeled cells were placed on ice, washed with cold physiologic salt buffer (PSB: 50 mM HEPES, [pH 7.4], 100 mM KAc, 2 mM $MgAc_2$) and then incubated with or without 50 μg/ml digitonin in PSB for 10 min on ice. Cells were washed another time with PSB and then harvested in 1% SDS, 0.1 M Tris, pH 8.0 and processed as above. With the exception of the CaM inhibitors, labeling efficiency was always verified to be equal among all samples by autoradiography of total lysates. Loading of all IP gels was verified to be equal by coomassie staining to visualize recovered IgG. Quantification of autoradiographs to measure the effect of CaM inhibition was done by phosphorimaging on a Typhoon scanner.

Protein Purification

pRSET-A or pGEX 6P-1 expression plasmids were transformed into BL21 (DE3) *E. coli* cells for the expression and purification of recombinant BirA (for in vitro biotinylation studies), HA-CaM (for addback experiments), GST (as a depletion control), GST-CaM (for transfer assays), and GST-CBP (for depletion of CaM). Cells were grown to log phase and induced with 1 mM IPTG for 4 hr at 37°C before they were harvested by centrifugation. Cell pellets were washed and resuspended in bacterial lysis buffer (50 mM HEPES or Tris [pH 7.5], 300 mM NaCl, 0.5 mM PMSF) with 10 mM imidazole for His-tagged proteins and lysed by a microfluidizer. Lysates were spun at 17,000 rpm for 30 min at 4°C in a JA-17 rotor to remove insoluble material. The supernatant was passed either over an immobilized Co^{2+} column (if His-tagged) or a glutathione-sepharose column (if GST-tagged), washed with bacterial lysis buffer that contained 20 mM imidazole for His-tagged proteins, and then eluted with either 100–250 mM imidazole (if His-tagged) or 10-25 mM reduced glutathione (if GST-tagged), with the exception of GST and GST-CBP used for depletion studies (see below). Eluted proteins were subsequently dialyzed into PSB.

In Vitro Translation and Translocation

In vitro transcription and translation in RRL and Fr-RRL (described below) in the presence of ^{35}S-methionine were as described before for 30 min at 32°C (Stefanovic and Hegde, 2007; Hessa et al., 2011; Sharma et al., 2010). Translation in N-RRL was the same as in RRL except that the translation extract was made with a completely 'native' RRL (i.e., nonnucleased and nonhemin treated). Final concentrations of all other additives remain the same. Thus, N-RRL contains the endogenous level of cytosolic Ca^{2+} derived from the reticulocyte cytosol, and any trace amounts contributed by the water and other shelf chemicals. Cotranslational translocation assays into RMs have been described previously (Fons et al., 2003). For posttranslational translocation assays, translation was terminated by either adding 10 μg/ml RNase A and/or by removing of ribosomes by ultracentrifugation (70,000 rpm in the TLA120.1 rotor (Beckman) for 30 min at 4°C). Translocation was initiated by adding RMs (derived from either canine or porcine pancreas; Walter and Blobel, 1983). The addition of recombinant proteins and calcium and EGTA manipulations were as described in the individual figure legends. Unless otherwise noted, translocation assays were for 30 min at 32°C, except for those shown in Figure 7C, which were conducted at 37°C. Protease protection assay for translocated products was as before (Stefanovic and Hegde, 2007; Fons et al., 2003). For immunoprecipitations or pulldowns, samples were first denatured by boiling to 100°C in 1% SDS, 0.1 M Tris, pH 8, then treated as described above for IPs or pulldowns from cultured cells. Translocation efficiencies were quantified with either Image J or by phosphorimaging using a Typhoon scanner. All band intensities were subtracted of background intensities and normalized for the number of methionines expected to be in the products. Translocation efficiencies were defined as the amount of signal-cleaved product divided by the sum of full-length and signal-cleaved products in a particular translocation reaction.

Fractionation of RRL

Fr-RRL was typically prepared from 25 ml RRL (from Green Hectares). Its characterization will be described in a future publication, but its preparation is as follows. All procedures were on ice or at 4°C. The lysate was centrifuged at 100,000 rpm for 40 min in the TLA100.4 rotor (Beckman). The supernatants were pooled, and the tubes rinsed (without disrupting the ribosomal pellet) with an equal volume of column buffer (20 mM Tris, [pH 7.5], 20 mM KCl, 0.1 mM EDTA, 10% glycerol), which was added to the supernatant. The pellet was resuspended by dounce homogenization in ribosome wash buffer (RWB: 20 mM HEPES, [pH 7.5], 100 mM KAc, 1.5 mM $MgAc_2$, 0.1 mM EDTA), layered onto a 1 M sucrose cushion in RWB, and re-isolated by centrifugation at 100,000 rpm for 1 hr in the TLA100.4 rotor. The final pellet was resuspended in one-tenth the original lysate volume, and defined as native ribosomes. The ribosome-free supernatant from above was applied to a 10 ml DEAE column at a flow rate of ~1 ml/min, and washed with column buffer until the red hemoglobin was removed (~50 ml). The washed column was eluted in a single step with 50 ml of column buffer containing 300 mM KCl. The eluate was adjusted slowly with solid ammonium sulfate to 75% saturation (at 4°C) with constant stirring. After 1 hr of mixing, the precipitate was recovered by centrifugation at 15,000 rpm in the JA-17 rotor. The supernatant was discarded and the pellet dissolved in a minimal volume (~8 ml) of dialysis buffer (20 mM HEPES, [pH 7.4], 100 mM KAc, 1.5 mM $MgAc_2$, 10% glycerol, 1 mM DTT). This was dialyzed against two changes of dialysis buffer overnight, recovered, adjusted to 10-12 ml (i.e., twice the original concentration), and flash-frozen in N_2. To make a translation competent Fr-RRL, the native ribosomes and dialyzed DEAE-eluate were adjusted to 72 mM KAc, 2.5 mM $MgAc_2$, 10 mM HEPES, (pH 7.4), 2 mM DTT, 0.2 mg/ml liver tRNA, 1 mM ATP, 1 mM GTP, 12 mM creatine phosphate, 40 μg/ml creatine kinase, 40 μM each amino acid (except Methionine), and 1 μCi/μl ^{35}S-Methionine. The concentration of ribosomes and lysate was the same as that of RRL.

Sucrose Gradients, Crosslinking, and Translocation

In most experiments, 200 μl translation reactions were layered on a 2 ml 5%–25% sucrose gradients in PSB and centrifuged for 5 hr at 55,000 rpm at 4°C in the TLS-55 rotor (Beckman). Eleven 200 μl fractions were then removed from the top. For translocation assays of sucrose gradient fractions, RMs were added (composing one tenth of the reaction volume), the reaction supplemented with an energy-regenerating system (1 mM ATP, 1 mM GTP, 10 mM Creatine phosphate, 40 μg/ml Creatine Kinase) and 1 mM DTT, and incubated for 30 min at 32°C. The remaining analysis was as above. Chemical crosslinking experiments of sucrose gradient fractions were performed with 250 μM DSS at room temperature for 30 min, quenched with 100 mM Tris, and samples were then subject to direct analysis or immunoprecipitation. For crosslinking of RRL, or N-RRL translation reactions, the samples were first diluted 10-fold in PSB (to dilute primary amines) before adding crosslinker as above. Fr-RRL was crosslinked directly since its buffer composition was known (see above) to lack primary amines. Photocrosslinking using benzophenone-modified or 4,4-azipentanoyl-modified lysyl-tRNA (from tRNA Probes) was as before (Do et al., 1996; Krieg et al., 1986), except Fr-RRL was used for the translation and the suppressor tRNA was included in the translation reaction at a final concentration of 1 μM. Both probes gave similar site-specific and crosslinking efficiency results. Crosslinking time courses were performed by rapidly freezing samples in liquid nitrogen at the indicated time points and UV irradiating on dry ice (Plath et al., 2004). Size fractionation of CecA and Prl in CaM-depleted lysates were on a 10%–50% sucrose gradient in physiologic salt buffer, centrifuged at 55,000 rpm for 1 hr at 4°C in the TLS-55 rotor, after which 200 μl fractions were collected and analyzed directly.

RM Treatments

For trypsin treatments, RMs were incubated with varying concentrations of trypsin at 4°C for 1 hr. Reactions were inactivated with an incubation with ten-fold excess of trypsin inhibitor followed by 2 mM PMSF at 4°C for 15 min. Treated RMs were then diluted two-fold in PSB, layered on a 300 μl 0.5 M sucrose cushion made in PSB, and spun at 70,000 rpm for 15 min in the TLA100.3 rotor. Reisolated

RMs were resuspended in membrane buffer (MB: 50 mM HEPES [pH 7.4], 250 mM sucrose, 100 mM KAc, 2 mM $MgAc_2$, 2 mM DTT). Lumenal proteins were removed by either mild detergent treatment or by high pH treatment. For detergent depletions, RMs were incubated in 50 mM HEPES pH 7.4, 250 mM sucrose, 2 mM DTT, 0.075% Deoxy Big CHAP (DBC) on ice for 15-30 min. LD-RMs were isolated by ultracentrifugation at 100,000 rpm for 15 min at 4°C in the TLA100.3 rotor. The pellet was resuspended in 50 mM HEPES (pH 7.4), 500 mM KAc, 5 mM $MgCl_2$, 250 mM sucrose, 2 mM DTT and DBC was added to 0.8% at twice the original volume of RMs, incubated on ice for 10 min, and ultracentrifuged at 100,000 rpn for 30 min in the TLA100.3 rotor. 200 μl of the supernatant was combined with 10 μl of 20 mg/ml lipids of phosphatidylcholine (PC) and phosphatidylethanolamine (PE) in a 4:1 PC:PE ratio that had been rehydrated in 50 mM HEPES (pH 7.4), 15% glycerol, 1 mM DTT. A small amount of rhodamine-labeled PE was also included to visibly label the proteoliposomes. The membrane protein/detergent/lipid mixture was then incubated with 100 mg Biobeads (Biorad) at 4°C for 12-18 hr with end-over-end mixing for detergent removal. The LD-RMs were separated from the Biobeads, diluted five-fold in cold H_2O, and the LD-RMs were isolated by ultracentrifugation at 70,000 rpm for 30 min at 4°C in a TLA100.3 rotor. The pellet containing LD-RMs was then resuspended in 20 μl of MB for every 100 μl starting RMs. To deplete lumenal contents with high pH, RMs were diluted ten-fold in 50 mM HEPES, 50 mM CAPS buffer adjusted to pH 7.5 or 9.5 and incubated on ice for 30 min. LD-RMs were isolated on a 300 μl 0.5 M sucrose cushion in PSB at 70,000 rpm for 15 min at 4°C and resuspended in MB. Isolation of RMs after translocation reactions were done on a 0.5 M sucrose cushion in PSB for 70,000 rpm for 10 min at 4°C in a TLA100.3 rotor.

Affinity Purification of CecA Associated Proteins

A procedure similar to earlier methods was employed (Stefanovic and Hegde, 2007). Briefly, 5 ml translation reaction of CecA in N-RRL with unlabeled methionine was centrifuged at 70,000 rpm for 30 min at 4°C in the TLA100.3 rotor (Beckman) to remove ribosomes. The supernatant was then passed over a 200 μl anti-3F4 antibody column, washed in PSB, and bound proteins eluted with 1 mM 3F4 peptide in PSB. Elutions were analyzed by SDS-PAGE and Coomassie staining or diluted and saved for immunoblotting analysis. The p20 band was excised, analyzed by mass spectrometry of tryptic digests (Midwest Bioservices), and matched to CaM with high confidence via three independent peptides.

Depletion and Addback of CaM

GST and GST-CBP were expressed in BL21 *E. coli*, bound to glutathione beads (GE Healthcare) and washed extensively with PSB. Gel-filtered N-RRL (to avoid elution with endogenous glutathione) was passed over the columns and the flow-through assembled into translation extracts (Sharma et al., 2010). Immunoblotting verified efficient depletion selectively of CaM, with no detectable change in any other proteins tested by blotting and coomassie staining. rCaM was expressed and purified from BL21 *E. coli* cells with a Co^{2+} column via its His tag as described above, eluted with 100 mM imidazole, and dialyzed into PSB for add-back into depleted lysates.

SUPPLEMENTAL REFERENCES

Ashok, A., and Hegde, R.S. (2008). Retrotranslocation of prion proteins from the ER by inhibition of GPI signal sequence transamidation. Mol. Biol. Cell *19*, 3463–3476.

Jungnickel, B., and Rapoport, T.A. (1995). A posttargeting signal sequence recognition event in the endoplasmic reticulum membrane. Cell *82*, 261–270.

Levine, C.G., Mitra, D., Sharma, A., Smith, C.L., and Hegde, R.S. (2005). The efficiency of protein compartmentalization into the secretory pathway. Mol. Biol. Cell *16*, 279–291.

Mariappan, M., Li, X., Stefanovic, S., Sharma, A., Mateja, A., Keenan, R.J., and Hegde, R.S. (2010). A ribosome-associating factor chaperones tail-anchored membrane proteins. Nature *466*, 1120–1124.

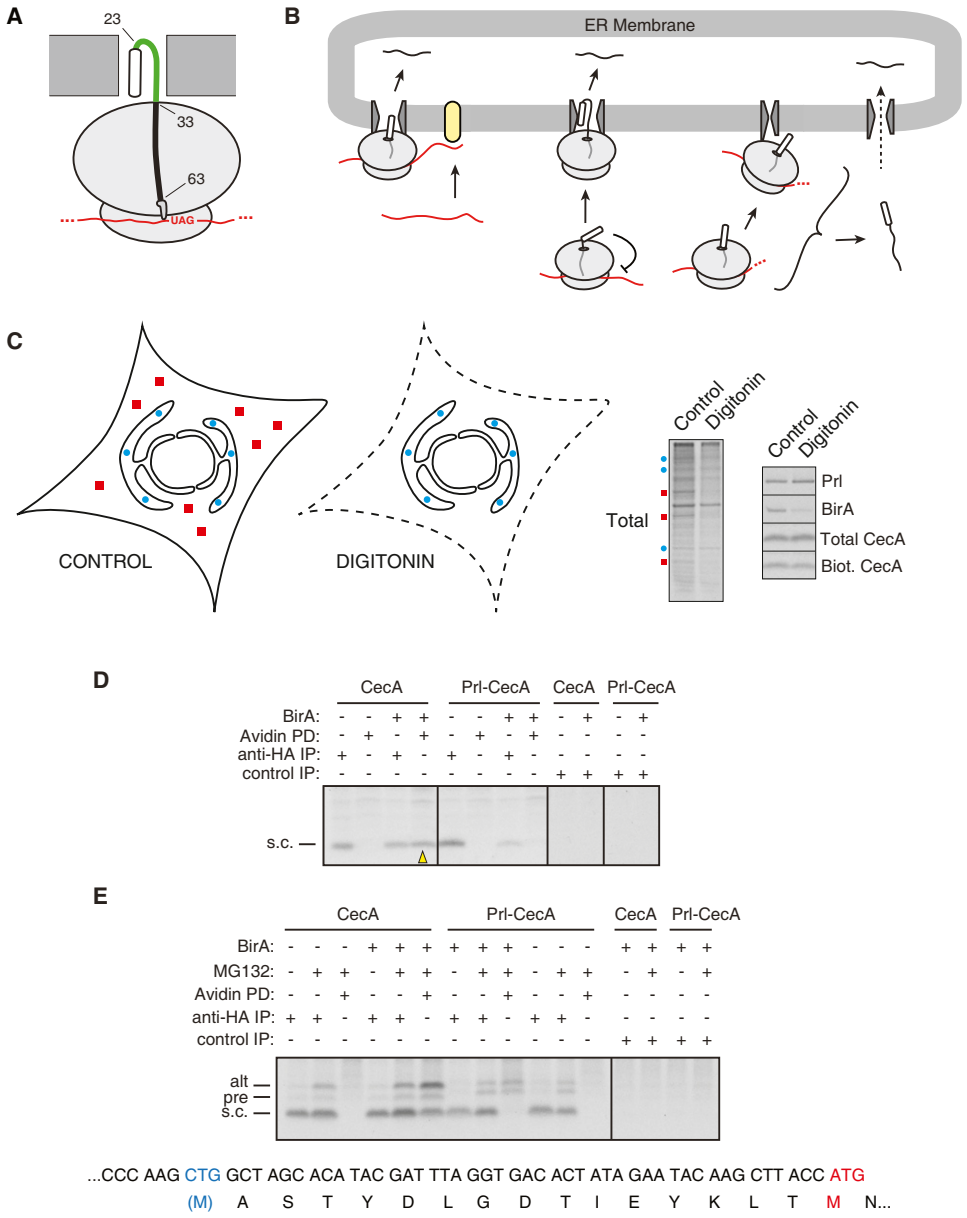

Figure S1. Posttranslational Translocation in Mammalian Cells, Related to Figure 1

(A) Architecture of a 63-residue nascent secretory protein. At least 30 residues of the nascent chain are buried inside the ribosome, leaving at most ~32 residues available to the cytosol. For an average signal sequence, this is the length at which SRP binds (Jungnickel and Rapoport, 1995) and has an opportunity to target to the ER. Even if the signal is relatively short (22 residues in the example shown), only ~10-12 residues would be left to traverse the distance (in green) from the ribosome tunnel exit to the lumenal face of the translocon to acquire the 'looped' orientation needed for translocation. The synthesis of 10–12 residues would also only allow a window of ~1–2.5 seconds (assuming a translation rate of 5–10 residues/second) for SRP to recognize and target the ribosome-nascent chain complex cotranslationally.

(B) Small-protein translocation could be facilitated by pre-targeting the mRNA to the membrane (via a hypothetical receptor, yellow) followed by translation by a translocon-bound ribosome (left diagram). Alternatively, the small protein could induce a sufficiently strong translational arrest to allow targeting (middle diagram). And finally, precursor released into the cytosol could access a posttranslational translocation pathway into the ER lumen (right diagram). Only the last model involves a fully cytosolically exposed intermediate, which is how we assay for posttranslational translocation. Models are not mutually exclusive.

(C) Subcellular fractionation to distinguish cytosolic from noncytosolic proteins (characterized in Levine et al., 2005). Left: diagram of assay, showing that 50 μg/ml digitonin selectively perforates the plasma membrane, releasing cytosolic proteins (red squares) while leaving organellar proteins intact (blue circles). HeLa cells were transfected with BioTagged CecA or BioTagged Prl with BirA, radiolabeled for 1 h, and treated on ice without or with digitonin. The cells were analyzed for total labeled proteins (Total), Prl, BirA, total CecA (recovered by anti-HA IPs), and biotinylated CecA (recovered by avidin pulldown). The total protein sample shows examples of extracted proteins (red squares) and retained proteins (blue circles). While BirA is efficiently extracted with digitonin, Prl, total CecA, and biotinylated CecA remain unaffected by digitonin, suggesting their localization to internal cellular organelles.

(D) HEK293T cells were transfected with BioTagged CecA or BioTagged Prl-CecA without or with cytosolic BirA, radiolabeled, and analyzed for biotinylated (i.e. cytosolically-exposed) and signal-cleaved (i.e. translocated) product (s.c.). This is observed with CecA (yellow arrowhead), indicating posttranslational translocation. By contrast, comparatively little Prl-CecA is biotinylated. Note that in contrast to HeLa cells, very little precursor is detected in HEK293T cells, perhaps due to faster translocation kinetics in this more highly secretory cell type.

(E) HeLa cells transfected with BioTagged CecA or BioTagged Prl-CecA without or with cytosolic BirA were treated with the proteasome inhibitor MG132, radiolabeled, and analyzed for total and biotinylated products. These constructs of BioTagged CecA and Prl-CecA contain an in-frame cryptic CTG start codon (blue) 16 codons upstream of the actual ATG start codon (red; see sequence at bottom). When translation initiates at this CTG codon, the hydrophobic signal sequence will be encoded in the middle of the protein, producing an alternative translation product ("alt") that is predominantly routed for proteasomal degradation in the cytosol. Accordingly, this alternative product is significantly stabilized with MG132, as is the Prl-CecA precursor. In contrast, the CecA precursor can be detected without MG132 and is only marginally stabilized with MG132. Note that the Prl-CecA precursor and Prl-CecA alternative product are slightly larger than the CecA precursor and CecA alternative product, respectively. This is due to 8 additional amino acids in the Prl signal sequence. That the "alt" product is derived from the cryptic CTG start site was verified by showing its disappearance upon mutation of the CTG (data not shown).

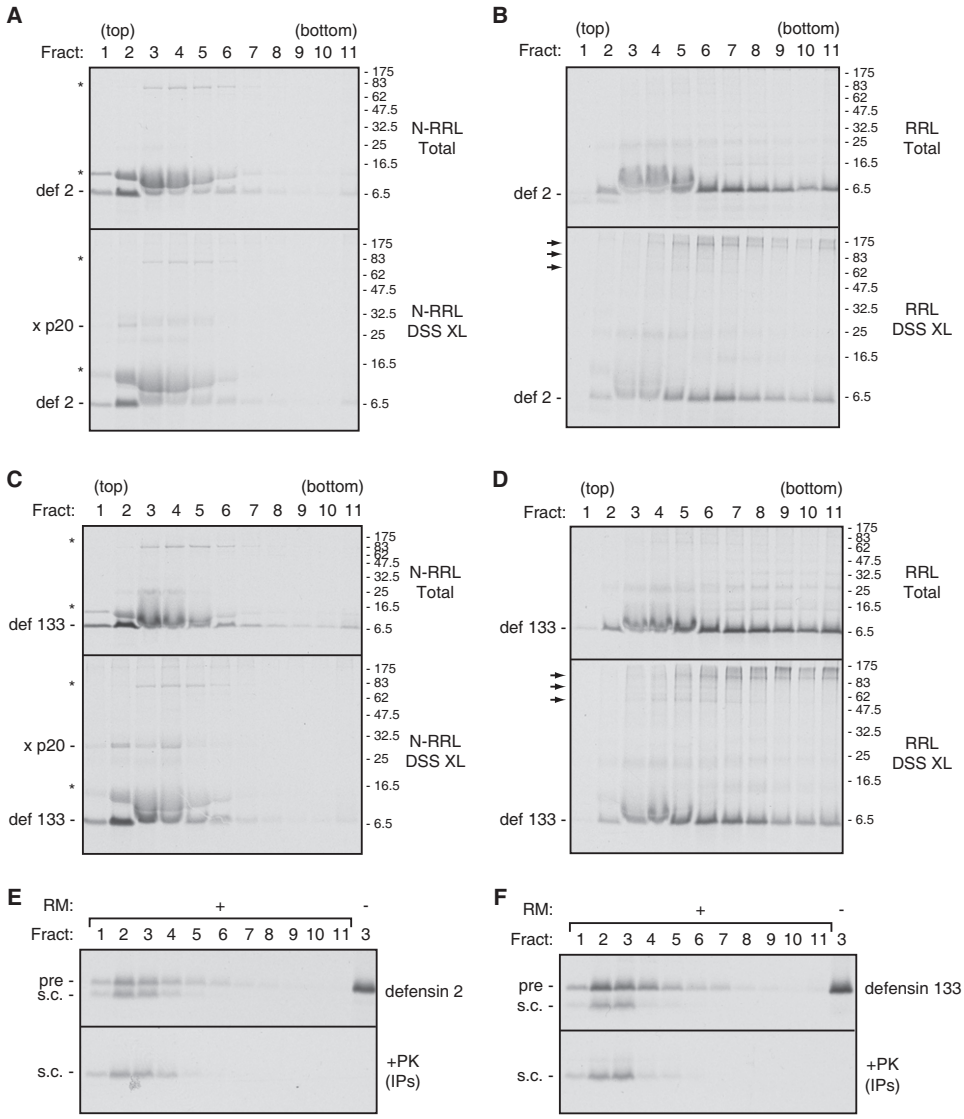

Figure S2. Analysis of Additional Small Secretory Proteins In Vitro, Related to Figure 2

(A, B, and E) The small secretory proteins beta-defensin 2 and (C, D, and F) beta-defensin 133 were translated in either N-RRL (A and C) or nucleased RRL (B and D), size fractionated on a 5–25% gradient (Total), and crosslinked with DSS (DSS XL). In N-RRL, both defensins migrate towards the top of the gradient and crosslinking reveals an interaction with a 20 kD partner. Asterisks mark proteins translated from endogenous mRNA in the lysate. In nucleased RRL, substrate distribution throughout the gradient is significantly more heterogeneous, and the interaction with p20 is lost and replaced by other proteins (arrowheads). (E and F) Individual fractions from N-RRL were also incubated with RMs (top) and subject to protease digestion (bottom). Both defensins can posttranslationally translocate in an RM-dependent manner, and their peak translocation activity and distribution throughout the sucrose gradient is similar to that of CecA in N-RRL.

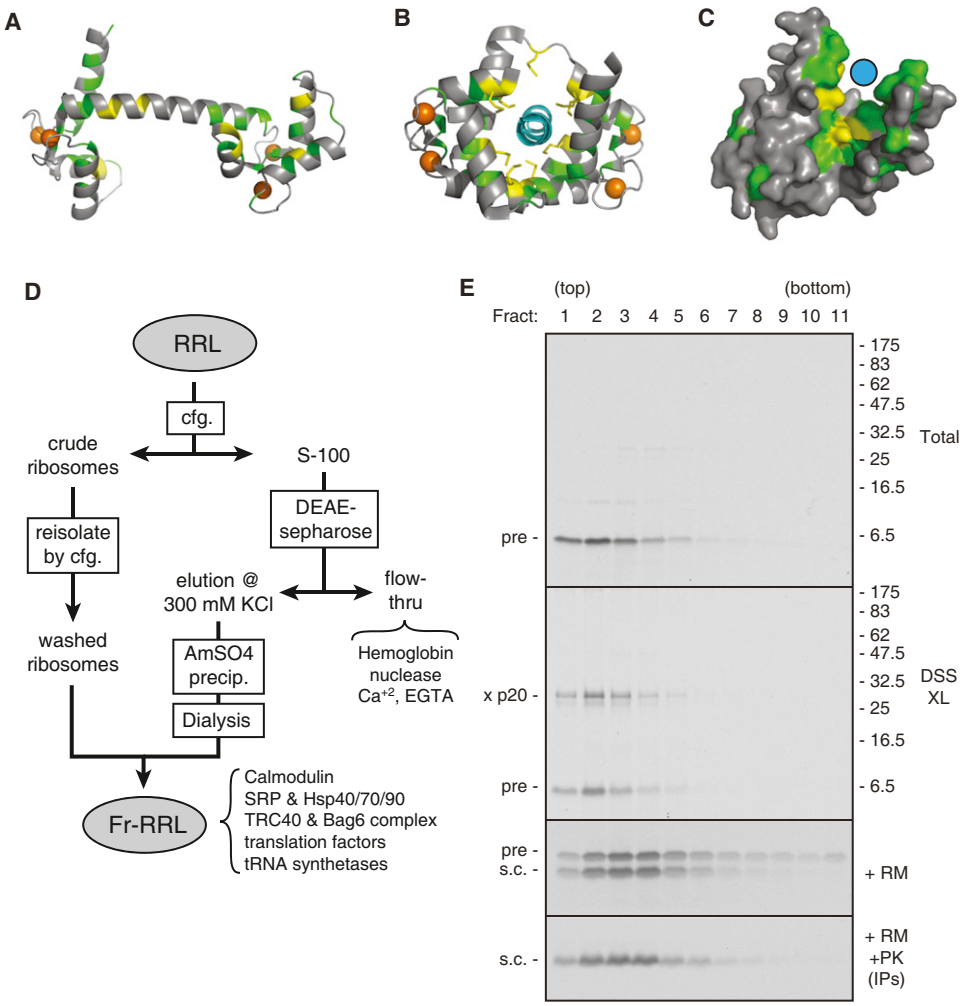

Figure S3. Related to Figure 4

(A–C) Structural comparison of CaM and SRP M-domain. Panel (A) shows CaM in an extended conformation (PDB ID 1CLL) with calcium ions in orange, methionine residues in yellow, and hydrophobic residues (V, I, L, F) in green. Panel (B) shows Calcium-bound CaM (PDB ID 1CDL) in a closed conformation bound to a target peptide (cyan). Methionine side chains are displayed. Panel (C) shows the signal sequence binding groove of SRP54 M-domain (PDB ID 2FFH) with hypothetical signal sequence shown in cyan. Like SRP, the binding groove of CaM is lined with hydrophobic amino acids and is rich in methionine residues, whose flexible chains can accommodate a diverse array of hydrophobic sequences.

(D) Schematic diagram of the fractionation procedure to produce Fr-RRL. Ribosomes are removed from RRL by centrifugation, washed, and added back to a DEAE-elution fraction. This system, when complemented with tRNAs, amino acids, and an energy regenerating system, is competent for translation. Indicated is a partial list of key factors verified (by blots and/or activity) to be in Fr-RRL, and those known to be lost in the DEAE flow thru fraction (most notably, EGTA and nuclease).

(E) CecA translated in Fr-RRL was size fractionated on a 5%–25% sucrose gradient (Total), revealing a significantly more homogenous distribution of CecA complexes than seen in conventional RRL translation systems (compare to Figure 2B). DSS crosslinking reveals that CecA primarily associates with p20 (DSS XL). Addition of RMs (+RMs) to individual gradient fractions and protease protection (+PK) reveals posttranslational translocation efficiencies of ~60% in the fractions where CecA interacts with p20.

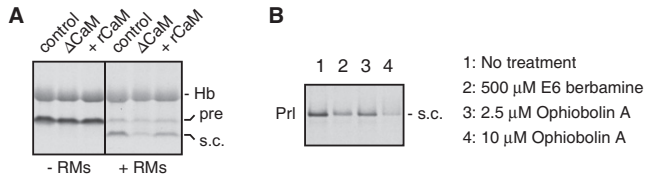

Figure S4. Related to Figure 5

(A) CaM depletion impairs small-protein translocation even under cotranslational conditions. CecA was translated in the absence of presence of RMs in N-RRL that was mock-depleted (control), CaM depleted (ΔCaM), or CaM depleted with recombinant HA-tagged CaM added back (+rCaM). Translation reactions were analysed directly by SDS-PAGE and autoradiography. Precursor (pre) and signal-cleaved (s.c.) CecA are indicated. Hb is hemoglobin. Even under these "co-translational" conditions where RMs are present during translation, CecA translocation is selectively impaired by the depletion of CaM and can be fully rescued by rCaM. The lower recovery of precursor upon CaM depletion is probably due to some ubiquitination of this failed translocation product in the absence of CaM (as illustrated in Figure 6D).

(B) CaM inhibitors do not inhibit Prl translocation in vivo. HeLa cells expressing Prl were pulse-labeled in the presence of the indicated CaM inhibitors. The Prl was immunoprecipitated and analyzed by SDS-PAGE. At inhibitor concentrations that have clear effects on CecA translocation, no precursor of Prl is detectable. The reduction in overall synthesis is due to a general effect on protein synthesis caused by CaM inhibition as judged by analysis of total cell lysates (data not shown). Note that MG132 was included during the labeling period to stabilize any precursor that might have accumulated. Experiments with a translocation inhibitor verified that precursor could have been detected had translocation been inhibited (data not shown).